Since the 1990s, ^{123}I-beta-methyl iodophenyl pentadecanoic (BMIPP) has been commercially available in Japan, where it has been extensively applied to the scintigraphic evaluation of various cardiac diseases [3]. BMIPP is a branched-chain fatty acid analog of *p*-iodophenyl pentadecanoic acid in which a methyl group added to the β-3 position inhibits mitochondrial β-oxidation. The rate of fatty acid metabolism is usually rapid and difficult to track, but BMIPP enables prolonged retention in the myocardium, a feature that is suitable for SPECT image acquisition [4].

BMIPP is clinically useful for detecting ischemia in patients with coronary artery disease and non-ischemic myocardial disease such as hypertrophic or dilated cardiomyopathy. Abnormal findings in BMIPP images might predict future cardiac events in patients with cardiomyopathy [5].

Cardiac imaging using BMIPP can sensitively detect myocardial ischemia and damage. Therefore, ischemic heart diseases are frequently visualized by dual isotope imaging with a myocardial perfusion tracer such as ^{201}thallium, or ^{99m}Tc-sestamibi (MIBI) [6]. Fatty acid metabolism is considered to decrease more rapidly than perfusion tracers when ischemia has occurred. Perfusion–metabolism mismatches are quite frequent in patients with ischemic heart disease [7, 8].

While many studies have examined the features and applications of BMIPP, some clinical reports have uncovered a controversial phenomenon [9]. Higuchi and Noriyasu et al. found in an animal experiment that the myocardial uptake of BMIPP is transiently accelerated during the very early phase of acute reperfusion ischemia compared with that of a perfusion tracer [10, 11]. These studies have visualized increased BMIPP uptake under acute reperfusion ischemia, but changes in the kinetics during this phenomenon remain unclear. Furthermore, to measure the precise kinetics of the tracer is difficult because of systemic effects (i.e. radioactivity in adjoining organs, systemic tracer recirculation, and hemodynamic influences). The present study aimed to elucidate the myocardial extraction and wash-out kinetics of BMIPP immediately after reperfusion ischemia in the isolated rat heart model.

Materials and methods

Preparation of radiopharmaceuticals

Nihon Medi-Physics Co. Ltd. (Kobe, Japan) supplied BMIPP (1 mg) in a kit and Fujifilm RI Pharma Co. Ltd. (Chiba, Japan) supplied MIBI (1 mg) in a lyophilized kit.

Experimental animals

Thirty-four male Wistar rats (body weight, 250–350 g; age, 6 weeks; Saitama Experimental Animals Co. Ltd, Saitama, Japan) were assigned to normal control (NG, $n = 6$), mildly ischemic (MG, $n = 5$) or severely ischemic (SG, $n = 5$) groups. The group assignment was similar for the MIBI kinetic study groups (NG, $n = 6$; MG, $n = 6$; SG, $n = 6$).

The heart was quickly isolated under deep anesthesia induced with an intraperitoneal injection of pentobarbiturate (25 mg/g), and the aorta was cannulated to initiate retrograde perfusion according to the Langendorff method (LE 05.200®; Panlab, Barcelona, Spain). A thermometer was inserted into the left ventricle of the isolated heart and connected with a thermostat (LE 13206 Thermostat Letica®, Barcelona, Spain) to measure and maintain the temperature of the chamber at 37°C. Circulation pressure and ECG were continuously monitored using an amplifier (Bio Amp®; Power Lab System AD Instruments, Barcelona, Spain). The isolated heart was perfused with Krebs–Henseleit bicarbonate buffer [g/L: D-glucose (2.0), magnesium sulfate (0.141), potassium phosphate monobasic (0.16), potassium chloride (0.35), and sodium chloride (6.9); SIGMA Chemical Co., St. Louis, MO, USA] containing $NaHCO_3$ 2.1 mg/L and $CaCl_2$ 0.175 mg/L. The buffer was continuously bubbled with 95% O_2/5% CO_2 throughout the study. The isolated heart was wrapped with Parafilm® to maintain the moisture content throughout the study and perfused with the buffer using a pump system (Miniplus3 Peristaltic Pump® and STH Pump Controller®; Gilson Inc., Middletown, WI, USA) at a constant flow rate of 10 mL/min. A Parafilm®-covered, external gamma probe (ALOKA Co., Ltd., Tokyo, Japan) connected to an analyzer (Gamma-Chaser®, ALOKA) was applied to whole hearts to determine radioactivity levels on a count-per-sec basis throughout the study.

Figure 1 shows the study protocol. Stabilization of the heart for 15 min achieved by perfusion with BMIPP or MIBI in the buffer at the above constant rate for 20 min was followed by 25 min of tracer-free wash-out. In the ischemia groups, global myocardial ischemia was induced by stopping pump infusion with perfusion medium (15 min for mild ischemia, and 30 min for severe ischemia) prior to tracer wash-in and out study. The same protocols were performed for both BMIPP and MIBI. The radioactivity in the buffer was determined using a gamma-well counter (Well Counter®, ALOKA). The calibration factor for the radioactivity between the buffer and heart was determined as described [12].

Sampling energy windows were set to 140–180 keV. Sampling data were recorded every second in the Excel format on a personal computer, and time–activity curves were generated using Excel®. All curves were corrected for

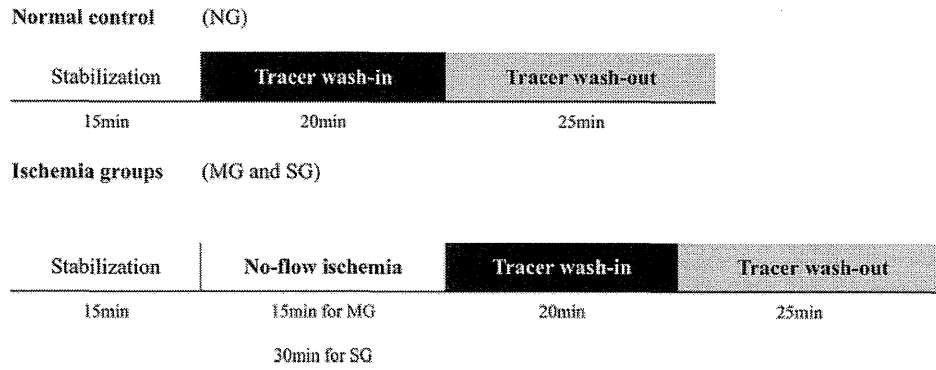

Fig. 1 Study protocols. After 15 min of stabilization, tracer (BMIPP or MIBI) wash-in of the rat heart proceeded for 20 min, followed by wash-out for 25 min. No-flow ischemia was implemented before these two studies. NG, MG and SG: control, mild and severe ischemia groups

radioactive decay, and we adopted a single-compartmental tracer kinetic model in which K_1 is described as flow velocity into myocardium, and k_2 as diffusion from myocardial cell and extra cellular space, namely myocardial wash out. Since flow in vessel should be constant due to continuous pump infusion (10 ml/min), K_1 was obviously defined as an extraction rate into myocardium. The principles and equation have been previously described [12].

Biochemical concentration

Effluent buffer from the rat heart was sampled at 10, 15 and 20 min during constant perfusion, and 10 ml of each sample was collected using EDTA tubes before measurements. Lactate was measured using lactate oxidase enzyme and visible spectrophotometry according to the Japanese Society of Laboratory Medicine. Mean values were calculated from sampled data in each group.

Statistical analysis

Values are expressed as mean values ± SD and were compared with nonparametric data by the Kruskal–Wallis and Mann–Whitney tests using StatView® (version 5.0, SAS Institute, NC) for Windows. A value of $p < 0.05$ was considered statistically significant.

Results

Hemodynamics during retrograde perfusion

The temperature of the left ventricle did not change significantly (36.6 ± 0.4°C; $n = 27$) in any of the groups, and oxygen saturation was at least 90% in all rats throughout the study. Table 1 shows significantly higher circulation pressure and a significantly lower heart rate in SG compared with NG and MG ($p < 0.05$, respectively).

Tracer kinetics

Figure 2 showed the K_1 value from the results. MIBI-K_1 was significantly decreased in the MG and SG groups compared with NG and MG groups, respectively, and SG also significantly differed among the groups (3.45 ± 1.10, 1.95 ± 0.82 and 1.05 ± 0.13 ml/min for NG, MG and SG, respectively; $p < 0.05$ for each). On the other hand, BMIPP-K_1 was significantly higher in the ischemic groups than in NG, and BMIPP-K_1 was significantly higher in SG than in MG (3.06 ± 0.88, 3.91 ± 0.87 and 4.94 ± 1.51 ml/min for NG, MG and SG, respectively; $p < 0.05$ for each).

An inverse relationship was observed between MIBI- and BMIPP-K_1 in ischemia groups, and a significantly higher ratio of metabolism-perfusion uptake (BMIPP-K_1/MIBI-K_1) was found according to ischemic severity (0.89 ± 0.25, 2.0 ± 0.44 and 4.70 ± 1.43 for NG, MG and SG, respectively; $p < 0.05$ for each comparison).

From the wash-out kinetics, MIBI-k_2 was markedly higher for SG than for MG and NG (0.00072 ± 0.0011, 0.00038 ± 0.00076 and 0.043 ± 0.033 for NG, MG and SG; $p < 0.05$ for SG vs. NG and MG), whereas BMIPP-k_2 did not significantly differ between any of the groups (0.0056 ± 0.0028, 0.0029 ± 0.0010 and 0.0037 ± 0.0022 for NG, MG and SG, respectively). As shown in Fig. 3, MIBI-k_2 showed a lower value compared to BMIPP, but was further accelerated in SG than in those of MIBI ($p < 0.05$).

Biochemical profile

Lactate was significantly increased in MG compared with NG (2.22 ± 0.62 and 0.53 ± 0.15 mg/dl, respectively; $p < 0.0001$) and tended to increase in SG (5.15 ± 3.12 mg/dl) compared with MG but the difference did not reach statistical significance.

Table 1 Hemodynamic parameters

Tracer		Normal control	Mild ischemia	Severe ischemia
Heart rate (min^{-1})	Rat $heart_{BMIPP}$	244 ± 76	304 ± 105	94 ± 140*
	Rat $heart_{MIBI}$	283 ± 90	290 ± 116	100 ± 123*
Circulation pressure (mmHg)	Rat $heart_{BMIPP}$	67 ± 13	101 ± 31	160 ± 84*
	Rat $heart_{MIBI}$	56 ± 20	93 ± 42	183 ± 70*

* $p < 0.05$ versus normal control and mild ischemia

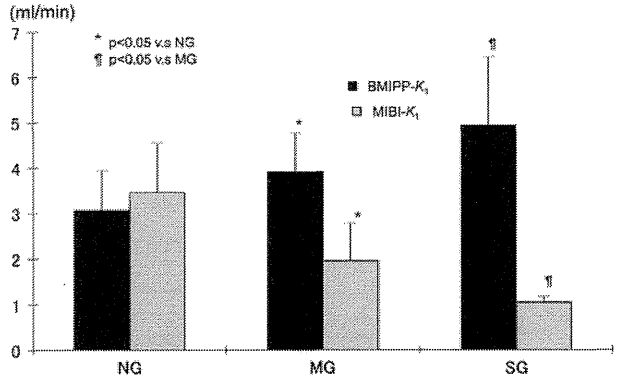

Fig. 2 Mean values ± SD for K_1 in each group. MIBI significantly decreased according to the duration of ischemia ($p < 0.05$ for NG versus MG and MG versus SG), whereas BMIPP significantly increased ($p < 0.05$ for NG versus MG and MG versus SG). NG, MG and SG: control, mild and severe ischemia groups

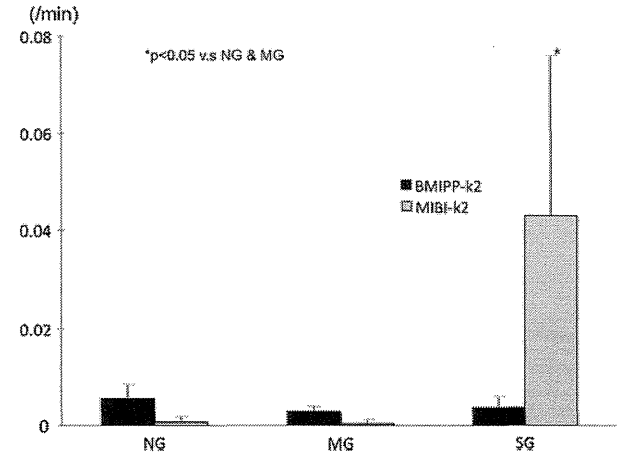

Fig. 3 Mean values ± SD for k_2 in each group. MIBI showed lower k_2 values in NG and MG, but significantly accelerated values in SG (3.45 ± 1.10, 1.95 ± 0.82, and 1.05 ± 0.13 ml/min for NG, MG and SG, respectively; $p < 0.01$ versus NG and MG). BMIPP showed comparable k_2 in all groups (3.06 ± 0.88, 3.91 ± 0.87 and 4.94 ± 1.51 ml/min for NG, MG, and SG)

Discussion

In the present study, we assessed the myocardial kinetics of BMIPP using the isolated rat heart model under acute reperfusion ischemia.

Myocardial perfusion uptake (MIBI-K_1) was significantly decreased in the mild ischemia group compared with the normal control, and further decreased in the groups with severe ischemia. In other words, deceased MIBI-K_1 reflected the severity of ischemia. These results are similar to those of a previous study using the same protocols in the same experimental setting [12]. Reperfused myocardium might become edematous during ischemia, with vascular beds becoming degraded so that myocardial flow decreased even after reperfusion.

In contrast to the kinetics of the perfusion tracer, BMIPP-K_1 was significantly increased with increasing duration of no-flow ischemia. This hemodynamic change followed by a reduction in MIBI extraction suggested that ischemic damage worsens in parallel with longer duration of ischemia, despite which BMIPP uptake increased. Myocardial fatty acid metabolism is promptly impaired under ischemic or hypoxic conditions. The changes in BMIPP uptake may be controversial, but some experimental evidence supports our findings. Higuchi and Noriyasu et al. found that BMIPP uptake increased during acute reperfusion ischemia in rats and persists for at least 48 h while myocardial perfusion decreased [10, 11]. Higuchi also investigated serial changes in BMIPP uptake over time and found that it decreased 3 days later. Miller found using a similar carbon labeled fatty acid analog that accelerated fatty acid metabolism might imply myocardial viability in the reperfused dog model in addition to small animals [13]. Renstrom et al. [14] reported that BMIPP uptake increases in hypoxic, compared with normal, pig models. While these studies have reported the phenomenon of increased BMIPP uptake after reperfusion for various animal models or serial time points, no studies have reported the change in the degrees of the duration of ischemia. Our study, to our knowledge, is the first to note increased BMIPP uptake in various durations of ischemia.

The metabolic fate of BMIPP is essentially similar to that of free fatty acids, which are thought to combine with fatty acid binding protein mediated by $CD36^+$ on the myocardial cell membrane, and then become transported into the triglyceride pool and mitochondria in the activated

form with acyl-CoA. Over half of the myocardial BMIPP is stored in the triglyceride pool and 15% is consumed in mitochondria [15, 16]. This process is distinct from endogenous free fatty acid metabolism. Morishita et al. [17] reported that BMIPP uptake is increased in the triglyceride pool and that its metabolite is decreased during low-flow ischemia and hypoxia in the isolated rat heart model. Saddik and Lopaschuk et al. reported that triglyceride synthesis significantly increases in the isolated rat heart model under reperfusion ischemia [18, 19]. Other investigators have speculated that $CD36^+$ on the myocardial membrane regulates and enhances the rate of fatty acid uptake and triacylglycerol esterification [20–22].

Several investigators contend that MIBI clearance is a useful marker of myocardial mitochondrial dysfunction [23–25]. We found here that the MIBI-k_2 increased in severe ischemia reperfusion whereas the BMIPP-k_2 did not. Hosokawa et al. [7] reported that the early phase of myocardial extraction and BMIPP clearance are frequently affected by a flood of non-metabolized BMIPP from the myocardium, which is referred to as back diffusion. They also found that back diffusion increases soon after reperfusion–ischemia and persists for 3–5 min in the canine model. Here, we maintained rat hearts under constant perfusion for over 20 min of wash-in and wash-out, and so we considered that back diffusion might not affect the calculated K_1 and k_2 values. The constant k_2 value in the ischemia groups implies the stable retention of BMIPP metabolites. Considering myocardial mitochondrial dysfunction indicated by the accelerated MIBI wash-out, the increased BMIPP uptake immediately after reperfusion is probably caused by an accelerated fatty acid transport system due to an expanded triglyceride pool. This phenomenon may be explained by physiologic properties of BMIPP, which was designed for stable retention in the triglyceride pool.

Several clinical reports have captured the increased BMIPP uptake in acute ischemia [26, 27], but it has been widely acknowledged that BMIPP uptake is reduced after myocardial ischemia either reperfused or not. And this might raise a question of the discrepancy between clinical experience and the results from experimental research including the present study. Several factors might be involved: (1) Species variability should be noticed. 2) Most fatty acid imaging studies are performed at a minimum of several hours after onset of acute coronary occlusion or/and reperfusion. This might be too late to visualize the alteration of BMIPP uptake on a minute-by-minute basis in the quite early phase of acute ischemia in man. (3) There are possibilities that fatty acid metabolism may be impaired as a result of occult and repeatable ischemia that is characterized by flow impairment in coronary artery disease [28], and it is unknown how fatty acid metabolism alters in the initial exposure to myocardial ischemia.

However, various alterations of BMIPP have been speculated, which may imply that the results from the present study might reflect a possible phenomenon. In conclusion, this is the first study to determine the phenomenon of increased uptake rate of BMIPP immediately after reperfusion ischemia from the viewpoint of tracer kinetics. BMIPP uptake increased and wash-out did not vary with decreased perfusion after no-flow ischemia. Further studies are therefore required to explore the discrepancy between BMIPP kinetics and true fatty acid metabolism under ischemic conditions.

Study limitations

Our perfusion system was not truly equivalent to coronary perfusion because it provided retrograde constant perfusion and did not provide physiological, systemic recirculation. Yamamichi [29] described that fatty acid metabolism would change according to the composition of the perfusion medium such as other fatty acids and albumin. However, we found no changes in BMIPP-K_1 between buffers with or without oleic acid and albumin (data not shown). As the rats were fed with a normal diet up until the time of sacrifice, the notion that stored fatty acid in myocardium had become depleted is difficult to accept. Even though myocardial fatty acid metabolism might depend on systemic energy consumption, the isolated heart system precludes the effects of radioactivity from proximal organs and enables measurements of tracer kinetics that would not be affected by recirculation.

Conclusion

BMIPP uptake increased immediately after reperfusion ischemia, and this phenomenon was mediated not by altering clearance but by accelerating extraction. Fatty acid uptake might become transiently accelerated during the hyperacute phase of reperfusion ischemia.

Acknowledgment We are grateful to Nihon-mediphysics and Fujifilm RI Pharma for continuous donations of BMIPP and MIBI.

Conflict of interest We declare no conflict of interest in connection with this paper.

References

1. Barger PM, Kelly DP. PPAR signaling in the control of cardiac energy metabolism. Trends Cardiovasc Med. 2000;10(6):238–45.

2. Goodwin GW, Taylor CS, Taegtmeyer H. Regulation of energy metabolism of the heart during acute increase in heart work. J Biol Chem. 1998;273(45):29530–9.
3. Tamaki N, Morita K, Kawai Y. The Japanese experience with metabolic imaging in the clinical setting. J Nucl Cardiol. 2007;14(Suppl 3):S145–52.
4. Tamaki N, Kawamoto M. The use of iodinated free fatty acids for assessing fatty acid metabolism. J Nucl Cardiol. 1994;1(2 Pt 2):S72–8.
5. Yazaki Y, Isobe M, Takahashi W, et al. Assessment of myocardial fatty acid metabolic abnormalities in patients with idiopathic dilated cardiomyopathy using 123I BMIPP SPECT: correlation with clinicopathological findings and clinical course. Heart. 1999;81(2):153–9.
6. Nakamura A, Momose M, Kondo C, Nakajima T, Kusakabe K, Hagiwara N. Ability of (201)Tl and (123)I-BMIPP mismatch to diagnose myocardial ischemia in patients with suspected coronary artery disease. Ann Nucl Med. 2009;23(9):793–8.
7. Hosokawa R, Nohara R, Fujibayashi Y, et al. Myocardial metabolism of 123I-BMIPP in a canine model with ischemia: implications of perfusion–metabolism mismatch on SPECT images in patients with ischemic heart disease. J Nucl Med. 1999;40(3):471–8.
8. Kawai Y, Tsukamoto E, Nozaki Y, Morita K, Sakurai M, Tamaki N. Significance of reduced uptake of iodinated fatty acid analogue for the evaluation of patients with acute chest pain. J Am Coll Cardiol. 2001;38(7):1888–94.
9. Sloof GW, Visser FC, Bax JJ, et al. Increased uptake of iodine-123-BMIPP in chronic ischemic heart disease: comparison with fluorine-18-FDG SPECT. J Nucl Med. 1998;39(2):255–60.
10. Higuchi T, Taki J, Nakajima K, Kinuya S, Namura M, Tonami N. Time course of discordant BMIPP and thallium uptake after ischemia and reperfusion in a rat model. J Nucl Med. 2005;46(1):172–5.
11. Noriyasu K, Mabuchi M, Kuge Y, et al. Serial changes in BMIPP uptake in relation to thallium uptake in the rat myocardium after ischaemia. Eur J Nucl Med Mol Imaging. 2003;30(12):1644–50.
12. Fukushima K, Momose M, Kondo C, Kusakabe K, Kasanuki H. Myocardial kinetics of (201)Thallium, (99m)Tc-tetrofosmin, and (99m)Tc-sestamibi in an acute ischemia-reperfusion model using isolated rat heart. Ann Nucl Med. 2007;21(5):267–73.
13. Miller DD, Gill JB, Livni E, et al. Fatty acid analogue accumulation: a marker of myocyte viability in ischemic-reperfused myocardium. Circ Res. 1988;63(4):681–92.
14. Renstrom B, Rommelfanger S, Stone CK, et al. Comparison of fatty acid tracers FTHA and BMIPP during myocardial ischemia and hypoxia. J Nucl Med. 1998;39(10):1684–9.
15. Knapp FF Jr, Kropp J. Iodine-123-labelled fatty acids for myocardial single-photon emission tomography: current status and future perspectives. Eur J Nucl Med. 1995;22(4):361–81.
16. Nohara R. Lipid metabolism in the heart—contribution of BMIPP to the diseased heart. Ann Nucl Med. 2001;15(5):403–9.
17. Morishita S, Kusuoka H, Yamamichi Y, Suzuki N, Kurami M, Nishimura T. Kinetics of radioiodinated species in subcellular fractions from rat hearts following administration of iodine-123-labelled 15-(*p*-iodophenyl)-3-(*R*,*S*)-methylpentadecanoic acid (123I-BMIPP). Eur J Nucl Med. 1996;23(4):383–9.
18. Lopaschuk GD, Spafford MA, Davies NJ, Wall SR. Glucose and palmitate oxidation in isolated working rat hearts reperfused after a period of transient global ischemia. Circ Res. 1990;66(2):546–53.
19. Saddik M, Lopaschuk GD. Myocardial triglyceride turnover during reperfusion of isolated rat hearts subjected to a transient period of global ischemia. J Biol Chem. 1992;267(6):3825–31.
20. Coort SL, Hasselbaink DM, Koonen DP, et al. Enhanced sarcolemmal FAT/CD36 content and triacylglycerol storage in cardiac myocytes from obese zucker rats. Diabetes. 2004;53(7):1655–63.
21. Glatz JF, Bonen A, Ouwens DM, Luiken JJ. Regulation of sarcolemmal transport of substrates in the healthy and diseased heart. Cardiovasc Drugs Ther. 2006;20(6):471–6.
22. Luiken JJ, Arumugam Y, Dyck DJ, et al. Increased rates of fatty acid uptake and plasmalemmal fatty acid transporters in obese Zucker rats. J Biol Chem. 2001;276(44):40567–73.
23. Arbab AS, Koizumi K, Toyama K, Arai T, Araki T. Technetium-99m-tetrofosmin, technetium-99m-MIBI and thallium-201 uptake in rat myocardial cells. J Nucl Med. 1998;39(2):266–71.
24. Ayalew A, Marie PY, Menu P, et al. (201)Tl and (99m)Tc-MIBI retention in an isolated heart model of low-flow ischemia and stunning: evidence of negligible impact of myocyte metabolism on tracer kinetics. J Nucl Med. 2002;43(4):566–74.
25. Kailasnath P, Sinusas AJ. Technetium-99m-labeled myocardial perfusion agents: are they better than thallium-201? Cardiol Rev. 2001;9(3):160–72.
26. Nishikawa S, Ito K, Takada H, et al. Increasing myocardial 123I-BMIPP uptake in non-ischemic area in a patient with acute myocardial ischemia. Ann Nucl Med. 2002;16(8):573–6.
27. Zen K, Ito K, Hikosaka T, et al. Uncommon and dynamic changes detected by 123I-15-(*p*-iodophenyl)-3-*R*,*S*-methylpentadecanoic acid myocardial single photon emission computed tomography in a stunned myocardium induced by coronary microvascular spasm. Ann Nucl Med. 2000;14(4):303–9.
28. Kageyama H, Morita K, Katoh C, et al. Reduced 123I-BMIPP uptake implies decreased myocardial flow reserve in patients with chronic stable angina. Eur J Nucl Med Mol Imaging. 2006;33(1):6–12.
29. Yamamichi Y, Kusuoka H, Morishita K, et al. Metabolism of iodine-123-BMIPP in perfused rat hearts. J Nucl Med. 1995;36(6):1043–50.

Heart Vessels (2011) 26:582–589
DOI 10.1007/s00380-010-0110-4

ORIGINAL ARTICLE

Efficacy of paclitaxel-eluting stent implantation in hemodialysis patients

Michiaki Higashitani · Fumiaki Mori · Norihiro Yamada · Hiroyuki Arashi · Asako Kojika · Hiromi Hoshi · Yuichiro Minami · Junichi Yamaguchi · Takao Yamauchi · Atsushi Takagi · Hiroshi Ogawa · Nobuhisa Hagiwara

Received: 13 July 2010 / Accepted: 3 December 2010 / Published online: 26 January 2011

Abstract Hemodialysis patients were recognized as a high-risk group for restenosis after percutaneous coronary intervention in the era of the bare-metal stent. Recently, sirolimus-eluting stents (SES) have reduced restenosis and target lesion revascularization (TLR); however, it has been reported that their efficacy in hemodialysis patients is limited. The purpose of this study was to investigate whether paclitaxel-eluting stents (PES) improved angiographic outcomes of hemodialysis patients compared with SES. This study is a retrospective cohort study. We analyzed 54 hemodialysis patients with 87 lesions implanted with PES from February 2007 to September 2008, and 49 hemodialysis patients with 68 lesions implanted with SES from August 2004 to January 2007. Angiographic follow-up after 8–10 months was obtained for 59 lesions (67.8%) in the PES group and 43 lesions (63.2%) in the SES group. At baseline, the PES patients had more peripheral artery disease compared with the SES group (66.7 vs. 34.7%; $p = 0.0012$). There were no significant differences in the angiographic characteristics or procedural index. The binary restenosis rate was lower in lesions implanted with PES than in those with SES (13.6 vs. 39.5%; $p = 0.034$). Accordingly, the TLR rate was lower in lesions implanted with PES than with SES (9.3 vs. 26.5%; $p = 0.041$). Our results suggest that PES is more effective than SES in reducing restenosis and TLR in hemodialysis patients.

M. Higashitani (✉) · F. Mori · N. Yamada · H. Arashi · A. Kojika · H. Hoshi · Y. Minami · J. Yamaguchi · T. Yamauchi · A. Takagi · H. Ogawa · N. Hagiwara
Department of Cardiology, Tokyo Women's Medical University, 8-1 Kawada-cho, Shinjuku-ku, Tokyo 160-0022, Japan
e-mail: mhigasit@hij.twmu.ac.jp

Keywords Drug-eluting stents · Hemodialysis · Percutaneous coronary intervention · Paclitaxel-eluting stents

Introduction

Drug-eluting stents (DES) have been hailed as an effective means to prevent restenosis after percutaneous coronary intervention (PCI). A significant reduction in major adverse cardiac events (MACE) and restenosis with DES were found in a meta-analysis [1, 2]. Renal insufficiency is an independent predictor of mortality after PCI [3, 4]. DES implantation for de novo coronary lesions in patients with mildly impaired renal function reduced clinical events compared with bare metal stent (BMS) implantation [5], whereas DES showed no benefit over BMS in patients with moderate to severe renal insufficiency [5, 6]. In Japan, cardiac disease is the leading cause of death among hemodialysis patients, accounting for about 30% of all-cause deaths [7]. Among hemodialysis patients with coronary artery disease (CAD), the cardiac survival rate was significantly higher in a PCI group than in a medication group [8]. These results suggested that dialysis patients who have a higher risk of CAD should undergo more aggressive treatment with PCI than was previously considered [8]. However, the effectiveness of DES implantation for a subset of patients on hemodialysis therapy for end-stage renal disease has not been fully investigated because many clinical randomized trials excluded this subset of patients. Recently, sirolimus-eluting stents (SES) were found to markedly reduce restenosis and target lesion revascularization (TLR) compared with BMS[1, 2]; however, it has been reported that their efficacy in patients with hemodialysis was limited [9–12]. The purpose of this study

was to evaluate the clinical and angiographic efficacy of the polymer-based paclitaxel-eluting stents (PES) compared with SES in hemodialysis patients.

Methods

Patient population

Since May 2007, it has been the policy in our institution to use PES in hemodialysis patients for PCI, except for patients with intolerance to antiplatelet therapy, planned surgery within 3 months requiring withdrawal of antiplatelet therapy, or inappropriate vessel size for the available PES in Japan. The study population consisted of 103 consecutive hemodialysis patients with 155 lesions. A total of 54 hemodialysis patients with 87 lesions were treated with PES between May 2007 and December 2008 (PES group). As a control group, we selected 49 consecutive hemodialysis patients with 67 lesions who were treated with SES from August 2004 to April 2007 before the approval of PES (SES group).

PCI

Lesions were treated using standard interventional techniques. In Japan, PESs were available in diameters of 2.5–3.5 mm and lengths of 8–32 mm. Predilatation and postdilatation were allowed at the discretion of the operators. Intravenous boluses of heparin were administered to maintain an activated clotting time that exceeded 250 s during the procedure. Treatment with aspirin, 81–100 mg/day, was started before the procedure and continued permanently. Ticlopidine 200 mg/day or clopidogrel 75 mg/day was prescribed for a minimum of 6 months after the procedure. In cases of intolerance or allergy to ticlopidine or clopidogrel, cilostazol 200 mg/day was used as an alternative antiplatelet therapy.

Coronary lesion analysis

Lesions were classified according to the modified American Heart Association/American College of Cardiology (AHA/ACC) classification [13]. Assessments using quantitative coronary angiography (QCA) before the procedure, after the procedure, and during follow-up were performed using a computerized, automated, edge-detection algorithm (QAngioXA V7.1.40.0, Medis, Leiden, The Netherlands) [14], by experienced cardiologists blinded to the devices used and the clinical outcomes. A 5-mm vessel segment proximal and distal to the stenosis was used to calculate the average reference vessel diameter (RVD). Minimal lumen diameter (MLD) was measured within the stent (in-stent analysis) and within the segment, including 5 mm proximal and distal to the stent edge (in-segment analysis). Late lumen loss was defined as the difference between MLD after the procedure and MLD at 8–10 months' follow-up. The percentage of diameter stenosis was defined as [(MLD/reference vessel diameter) $\times$ 100]. Coronary artery calcification was assessed according to the presence of thick calcification on fluoroscopy or widespread superficial calcification on intravascular ultrasound.

Endpoint definitions and follow-up

The diagnosis of acute myocardial infarction (MI) included all patients with ST-elevation MI, which was defined as new ST-segment elevation on the electrocardiogram, and a creatinine kinase level more than twice normal. Stent thrombosis was analyzed retrospectively using the new definition of stent thrombosis generated by the Academic Research Consortium [15]. Consequently, stent thrombosis was classified as definite, probable, or possible. Deaths were classified as either cardiac or non-cardiac. Binary restenosis was considered as the occurrence of stenosis >50% of the diameter in the stented lesions. Late lumen loss was defined as MLD at follow-up minus post-procedural MLD measured by QCA. The angiographic patterns of restenosis were classified as focal, diffuse intra-stent, diffuse proliferative, and totally occluding [16]. Target lesion revascularization (TLR) was defined as any repeat PCI or surgical bypass of the original target lesion. The target lesion was considered to be the area covered by the stent plus 5-mm margins proximal and distal to the edges of the implanted stent. Composite MACE included all-cause death, MI, and TLR. All patients were asked to return for QCA between 8 and 10 months after the procedure or earlier if angina symptoms occurred. Clinical follow-up was obtained 12 months after the procedure. All patients provided written informed consent.

Statistical analysis

Continuous variables were presented as mean $\pm$ standard deviation and compared using Student's t test. Categorical variables were expressed as numbers and percentages and compared using the chi-square test or Fisher's exact test, as appropriate. Time-to-events estimates were evaluated using Kaplan-Meier methods and compared using the log-rank test. Univariate Cox regression analysis was performed to assess predictors of TLR and MACE after PCI. Included variables were patient-related factors listed in Table 1, and lesion and procedural characteristics listed in Table 2. The multivariate model included variables with $p \leq 0.20$ in univariate analysis. Multivariate analysis was performed using a Cox proportional hazards model with a stepwise

Table 1 Clinical characteristics

	PES ($n = 54$)	SES ($n = 49$)	p value
Age (years)	64 ± 10	65 ± 9	0.75
Male	41 (76%)	41 (84%)	0.47
Diabetes mellitus	41 (76%)	32 (65%)	0.24
Diabetes mellitus with insulin treatment	23 (43%)	14 (29%)	0.14
Hypertension	48 (89%)	43 (88%)	0.90
Hyperlipidemia	31 (57%)	22 (45%)	0.28
Current smoker	11 (20%)	19 (39%)	0.040
Family history of ischemic heart disease	6 (11%)	15 (31%)	0.027
Peripheral artery disease	36 (67%)	17 (35%)	<0.01
Duration of dialysis (years)	7.1 ± 5.2	8.7 ± 7.1	0.18
Unstable angina pectoris	21 (39%)	9 (18%)	0.38
MI	1 (2%)	5 (10%)	0.17
Previous cerebrovascular disease	9 (17%)	6 (12%)	0.72
Previous myocardial infarction	21 (39%)	19 (39%)	0.99
Previous PCI	24 (44%)	17 (35%)	0.31
Previous CABG	14 (26%)	12 (25%)	0.87
No. of diseased vessels	2.3 ± 0.8	2.2 ± 0.8	0.47
Left main coronary artery disease	20 (37%)	3 (6%)	<0.01
LVEF (%)	40 ± 12	46 ± 12	0.014
Low EF (<40%)	26 (48%)	16 (33%)	0.11

Values are number of patients (%) or mean ± SD

FH family history of ischemic heart disease, *PES* paclitaxel-eluting stents, *SES* sirolimus-eluting stents, *MI* myocardial infarction, *PCI* percutaneous coronary intervention, *CABG* coronary artery bypass grafting, *LVEF* left ventricular ejection fraction

Table 2 Angiographic and procedural characteristics

	PES ($n = 87$)	SES ($n = 68$)	p value
AHA/ACC types			
A	0	0	0.31
B1	7 (8%)	4 (6%)	
B2	57 (66%)	37 (54%)	
C	23 (26%)	27 (40%)	
Target vessel			
LAD	32 (37%)	26 (38%)	0.24
LCX	20 (23%)	12 (18%)	
RCA	25 (29%)	29 (43%)	
LMCA	6 (7%)	0	
SVG	0	0	
ITA	4 (5%)	1 (1%)	
Lesion characteristics			
Severe calcification	64 (74%)	46 (72%)	0.42
Ostial	19 (22%)	6 (9%)	0.049
Bifurcation	27 (31%)	19 (28%)	0.68
Chronic total occlusion	8 (9%)	1 (1%)	0.090
In-stent restenosis	7 (8%)	11 (16%)	0.19
Reference diameter (mm)	2.64 ± 0.77	2.86 ± 0.77	0.085
Minimum lumen diameter (mm)	0.88 ± 0.50	1.02 ± 0.47	0.066
Diameter stenosis (%)	68.0 ± 15.3	64.3 ± 13.3	0.11
Lesion length (mm)	23.9 ± 17.4	23.3 ± 14.5	0.80
Procedural characteristics			
No. of stents/lesion	1.4 ± 0.7	1.5 ± 0.8	0.56
Stent length (mm)	30.8 ± 20.0	34.5 ± 21.3	0.26
Stent diameter (mm)	3.1 ± 0.4	3.0 ± 0.4	0.15
Maximal dilatation pressure (atm)	15.4 ± 2.9	16.4 ± 3.5	0.047
Kissing balloon technique	21 (24%)	4 (6%)	<0.01
IVUS use	36 (41%)	22 (32%)	0.25
Rotational atherectomy	33 (38%)	20 (29%)	0.27

Values are number of lesions (%) or mean ± SD

ACC/AHA lesion class American College of Cardiology/American Heart Association lesion class, *PES* paclitaxel-eluting stents, *SES* sirolimus-eluting stents, *LAD* left anterior descending artery, *LCX* left circumflex artery, *RCA* right coronary artery, *LMCA* left main coronary artery, *SVG* saphenous vein graft, *ITA* internal thoracic artery

variable selection method. Hazard ratios were reported with 95% confidence intervals.

A p value <0.05 was considered significant. All statistical analyses were performed using SPSS version 16.0 (SPSS Inc., Chicago, IL) software for Windows (Microsoft Corp, Redmond, WA).

Results

Baseline patient, angiographic, and procedural characteristics

Baseline clinical characteristics are listed in Table 1. Current smoker and family history of ischemic heart disease were more frequent in the SES group ($p = 0.04$ and $p = 0.027$, respectively). Peripheral artery disease and left main CAD were more complicated in the PES group ($p < 0.001$ and $p < 0.001$, respectively). In addition, the left ventricular ejection fraction (LVEF) was lower in the PES group than in the SES group ($p = 0.014$). The prevalence of diabetes was as high as 70% in both groups. Diabetes showed an increased mortality following PCI [17]. Peripheral artery disease is common in hemodialysis patients and is associated with increased risk of cardiovascular mortality, morbidity, and hospitalization [18]. It was reported that LVEF reduction was an independent predictor of mortality in chronic kidney disease patients with CAD [19], and LVEF in the PES group of this study was lower compared with a previous report [9]. Duration of hemodialysis therapy in this study was about 7–9 years

longer than in a previous report of about 5 years [10]. We believe that this study population, especially the PES group, was clinically in a more critical state than previous study populations.

The prevalence of complex lesions (AHA/ACC B2/C) and severe calcification on angiography were similar in both the PES and SES groups. Compared with the SES group, the TLR rate and binary restenosis in the PES group were significantly lower. It was reported that the TLR rate was 12.0% and in-segment restenosis identified on follow-up angiography was 16.5% in diabetes patients implanted with PES [20]. Although this study population, undergoing hemodialysis, was more critical, the TLR rate was 9% and binary restenosis rate was 14%.

Their angiographic and procedural characteristics are listed in Table 2. No significant differences were observed between the two groups, but the PES group had more ostial lesions than the SES group ($p = 0.049$). In addition, the maximal dilatation pressure was higher in the SES group than in the PES group ($p = 0.047$). It is thought that this resulted from a difference in the stent balloons' nominal dilatation pressure, being higher for the SES balloon. The kissing balloon technique was performed more frequently in the PES group than in the SES group. Procedural success was achieved in all treated patients. There was no difference in the rate of rotational atherectomy use before stent placement between the two groups.

QCA analysis

Angiographic follow-up was obtained in 37 patients (68.5%) with 59 lesions in the PES group and in 33 patients (67.3%) with 43 lesions in the SES group. Serial QCA data are shown in Table 3. No significant difference was observed between the two groups before and after the procedure. However, the diameter of stenosis at follow-up and the angiographic binary restenosis rate were significantly lower in the PES group than in the SES group ($p = 0.028$ and $p = 0.034$, respectively). A pattern of focal restenosis was found in 82% of restenotic lesions treated with SES.

Type IC focal in-stent restenosis [16] was observed in half of the SES group and in none of the PES group with a pattern of focal restenosis in this study. In contrast, focal and diffuse patterns of restenosis were equal in patients treated with PES. However, a significant difference was not found between the two groups regarding focal or diffuse restenosis ($p = 0.16$).

Clinical follow-up outcomes

Clinical follow-up was obtained in all patients (Table 4). The TLR rate was significantly lower in the PES group (9%) than in the SES group (27%) ($p = 0.041$). No significant differences were observed between the two groups in all-cause death, cardiac death, MI, and MACE. In

Table 3 Serial quantitative coronary analysis data

	PES ($n = 59$)	SES ($n = 43$)	p value
Lesion follow-up rate	68%	63%	0.55
Lesion length (mm)	24.9 ± 18.7	24.0 ± 11.7	0.77
Preprocedure reference diameter (mm)	2.68 ± 0.72	2.83 ± 0.64	0.28
Minimal lumen diameter (mm) pre	0.89 ± 0.52	0.98 ± 0.47	0.36
Minimal lumen diameter (mm) post	2.89 ± 0.57	2.74 ± 0.58	0.21
Minimal lumen diameter (mm) follow-up	2.15 ± 0.75	1.95 ± 0.93	0.22
Late lumen loss	0.73 ± 0.83	0.79 ± 0.99	0.72
Diameter stenosis (%) pre	68.4 ± 15.5	66.1 ± 14.5	0.45
Diameter stenosis (%) post	10.6 ± 7.7	12.7 ± 9.9	0.23
Diameter stenosis (%) follow-up	27.1 ± 19.5	37.3 ± 26.7	0.028
Angiographic binary restenosis	8 (14%)	17 (40%)	0.034
Patterns of restenosis focal	4 (50%)	14 (82%)	0.16
I A	0	0	
I B	3	3	
I C	0	7	
I D	1	4	
Diffuse	4 (50%)	3 (18%)	0.16
II intra-stent	1	3	
III proliferative	3	0	
IV total occlusion	0	0	

Values are number of lesions (%) or mean ± SD

PES paclitaxel-eluting stents, *SES* sirolimus-eluting stents

Table 4 Major adverse cardiac events at 12 months

	PES ($n = 54$)	SES ($n = 49$)	p value
All-cause death	9 (17%)	8 (16%)	0.83
Cardiac death	4 (7%)	4 (8%)	0.82
Non cardiac death	5 (9%)	4 (8%)	0.88
Myocardial infarction	1 (2%)	4 (8%)	0.30
Target lesion revascularization	5 (9%)	13 (27%)	0.041
Composite major adverse cardiac events	15 (28%)	18 (37%)	0.33
Stent thrombosis	3 (6%)	3 (6%)	0.77
Definite	0	1	
Probable	0	0	
Possible	3	2	

Values are number of Patients (%)

PES paclitaxel-eluting stents, *SES* sirolimus-eluting stents

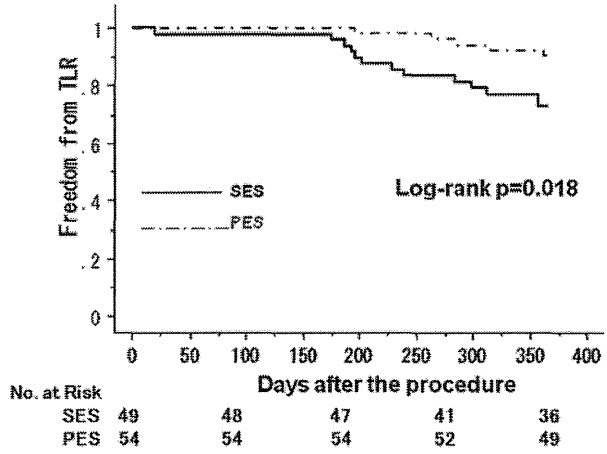

Fig. 1 Survival free from TLR in patients treated with SES versus PES from Kaplan-Meier estimates. PES, paclitaxel-eluting stents; SES, sirolimus-eluting stents

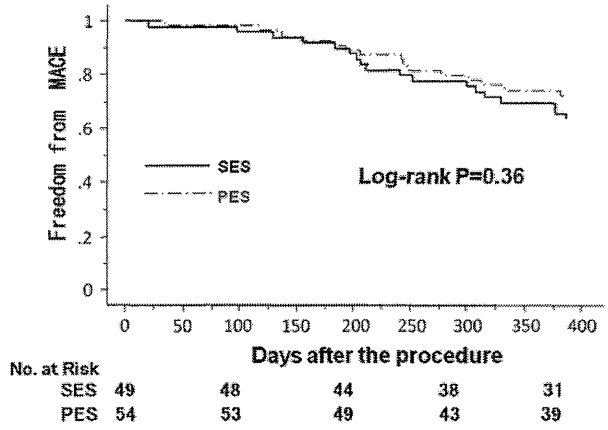

Fig. 2 Survival free from MACE in patients treated with SES versus PES from Kaplan-Meier estimates. PES, paclitaxel-eluting stents; SES, sirolimus-eluting stents

patients with cardiac death, two patients in the PES group and one in the SES group died of congestive heart failure, two patients in the PES group and one in the SES group suffered sudden death, one patient in the SES group died of acute MI, and one patient in the SES group died after stent thrombosis. The incidence of stent thrombosis at 1 year was 6% (3 cases) in the PES group and 6% (3 cases) in the SES group ($p = 0.77$). Of these cases, possible late stent thrombosis occurred in three patients in the PES group and in two patients in the SES group, and definite early stent thrombosis occurred in only one patient (2.0%) in the SES group and in none of the PES group. Kaplan-Meier curves of cumulative incidences of TLR are shown in Fig. 1. There was a significant difference in TLR (log-rank $p = 0.018$). Kaplan-Meier curves of cumulative incidences of MACE are shown in Fig. 2, and there was no statistical difference between the two groups (log-rank $p = 0.36$). Univariate Cox regression analysis to assess predictors of TLR showed two variables with $p \leq 0.2$. The variables were prior to MI and PES use, and were included in the multivariate Cox analysis. After adjusting for the variables, patients treated with PES had a significantly lower rate of TLR than those with SES (hazard ratio 0.29, 95% confidence interval 0.10–0.82, $p = 0.02$, Table 5). Univariate Cox regression analysis to assess predictors of MACE showed five variables with $p \leq 0.2$. The variables were prior MI, prior PCI, prior coronary artery bypass graft, LVEF, and duration of hemodialysis. These variables were included in the multivariate Cox analysis. After adjusting for the variables, duration of hemodialysis was the only significant predictor (hazard ratio 1.08, 95% confidence interval 1.02–1.15, $p < 0.01$, Table 6).

Discussion

The primary finding of this study was that treatment with PES was associated with a moderate reduction in TLR compared with SES in hemodialysis patients. To our knowledge these data are the first to compare PES versus SES outcomes in hemodialysis patients.

In this previous report, it was reported that the rate of MACE at 9 months in patients implanted with SES was significantly lower than in those implanted with PES (6.2% in the SES group and 10.8% in the PES group, $p = 0.009$) [21]. The difference was driven by a lower rate of TLR in the SES group than in the PES group (4.8 vs. 8.3%, $p = 0.03$). However, the risk of death was not significantly different between the PES group and the SES group [21, 22].

Recent studies in Japan in hemodialysis patients as a higher risk subset have reported that the TLR rate was similar between SES and BMS [9, 11, 12]. However, some studies have shown the efficacy of PCI using DES in dialysis patients with a similar reduction in repeat revascularization as in non-dialysis patients [23–25]. As discussed in those reports, a higher rate of angiographic follow-up may explain the increasing rate of TLR in Japan. In addition, different percentages of patients with complex and highly calcified lesions may contribute to the relatively high rate of TLR. Tamekiyo et al. [26] indicated that the studies in Japan included only SES [9, 11, 12], whereas other studies included SES and PES [23–25]. The different results in these studies may reflect a class side effect between the types of DES used in dialysis patients.

Two of the following are nominated for the reason why PES was effective than SES in this study. One reason is that the effectiveness of SES may attenuate in hemodialysis patients as a higher risk subset. The other reason is that

Table 5 Predictive factors for TLR at 12 months

Variables	Univariate analysis		*p*	Multivariate analysis		*p*
	Hazard ratio	95% Confidence interval		Hazard ratio	95% Confidence interval	
PES SES	0.31	0.11–0.87	0.03	0.29	0.10–0.82	0.02
Prior MI	0.36	0.14–0.94	0.04	0.34	0.13–0.88	0.03
Age	0.97	0.93–1.01	0.14			
Male	1.14	0.38–3.46	0.82			
Hypertension	0.98	0.38–1.15	0.38			
Hyperlipidemia	1.03	0.41–2.60	0.95			
Smoking	0.57	0.28–2.01	0.57			
FH	0.61	0.22–1.71	0.35			
Diabetes	1.27	0.48–3.39	0.63			
Peripheral artery disease	1.09	0.43–2.75	0.85			
LVEF	1.01	0.97–1.05	0.56			
Duration of dialysis	1.034	0.97–1.11	0.33			
Prior PCI	0.79	0.31–2.01	0.62			
Prior CABG	0.86	0.31–2.34	0.77			

Multivariate model includes variables with $p \leq 0.2$ in the univariate analysis

FH family history of ischemic heart disease, *PES* paclitaxel-eluting stents, *SES* sirolimus-eluting stents, *MI* myocardial infarction, *PCI* percutaneous coronary intervention, *CABG* coronary artery bypass grafting, *LVEF* left ventricular ejection fraction

Table 6 Predictive factors for MACE at 12 months

Variables	Univariate analysis		*p*	Multivariate analysis		*p*
	Hazard ratio	95% Confidence interval		Hazard ratio	95% confidence interval	
Duration of dialysis	1.09	1.03–1.15	<0.01	1.08	1.02–1.15	<0.01
Prior MI	0.53	0.27–1.04	0.06	0.73	0.34–1.54	0.4
Prior PCI	0.61	0.31–1.21	0.2	0.68	0.34–1.36	0.3
Prior CABG	0.59	0.29–1.22	0.2	0.79	0.36–1.73	0.6
LVEF	0.98	0.95–1.01	0.2	0.98	0.95–1.01	0.2
Age	1.00	0.97–1.04	0.86			
Male	0.91	0.40–2.04	0.81			
Hypertension	1.22	0.43–3.47	0.71			
Hyperlipidemia	1.26	0.63–2.49	0.52			
Smoking	1.36	0.61–3.02	0.45			
FH	0.99	0.40–2.12	0.85			
Diabetes	1.15	0.55–2.41	0.72			
Peripheral artery disease	0.88	0.44–1.74	0.71			
PES SES	0.36	0.37–1.44	0.73			

Multivariate model includes variables with $p \leq 0.2$ in the univariate analysis

FH family history of ischemic heart disease, *PES* paclitaxel-eluting stents, *SES* sirolimus-eluting stents, *MI* myocardial infarction, *PCI* percutaneous coronary intervention, *CABG* coronary artery bypass grafting, *LVEF* left ventricular ejection fraction

PESs show a similar effect in high risk subsets such as in this study. It is possible that the effectiveness of SES is limited in more complex and more highly calcified lesions for three possible reasons. First, the delivery of coronary stents through the rough surface of a calcified coronary artery lumen possibly strips off the polymer and drug of the SES [27]. Second, the recent imaging modality of optical coherence tomography has detected stent strut malapposition, which is a potential risk factor for restenosis or thrombosis after treatment of heavily calcified lesions,

despite the use of high-pressure dilatation or ROTA [28]. In fact, it was reported that the 2-year TLR rate was similarly high in a SES group and a BMS group treated with ROTA in dialysis patients (36 vs. 40%, $p = 0.55$) [26]. Third, the activities of sirolimus as preventing restenosis decrease in diabetic patients [29]. In this study, approximately 70% of patients had diabetes. Sirolimus and paclitaxel drugs activate mitogen-activated protein kinase pathways and inhibit mitogen-induced smooth muscle cell proliferation. Sirolimus potently activates AKT-dependent signaling, overriding the downregulation of this pathway by insulin resistance. This effect is associated with attenuation of the antimigratory effects of sirolimus in the presence of hyperglycemia, which might account for the decreased efficacy in diabetic patients compared with nondiabetic patients. On the other hand, paclitaxel inhibits restenosis independently of the pathways impacted in hyperglycemia [30]. In this theory PES may be more beneficial than SES for diabetic patients. In the SCAAR study [31], the sirolimus-eluting stent resulted in higher rates of restenosis in patients with diabetes compared with those in patients without diabetes. With the paclitaxel-eluting stent the incidence of restenosis was similar in patients with diabetes compared with that in patients without diabetes.

The study by Iakovou et al. [32] demonstrated that renal insufficiency was a key predictor of stent thrombosis in patients with DES implantation and that the incidence of stent thrombosis at 9 months after successful DES implantation in consecutive patients was 1.3%. In this study, the stent thrombosis rate was similar in the two groups and a little higher compared with a previous study in hemodialysis patients [9, 10]. The reason for this could be that the study population was more critical in this study than in previous studies.

In summary, the beneficial effect of SES may be reduced in patients with more complex lesions, whereas PES may be more effective than SES in patients with advanced disease such as that requiring hemodialysis. In this study, MACE occurred in about 30% of the PES group and is a high figure; thus, we have to examine optimal PCI and medical therapy, for example, aimed at further improvement in prognosis.

Study limitations

The study had four limitations. First, the study was limited by its small sample size, non-randomized nature, and performance at a single center. Second, this study comprised a retrospective analysis of a patient registry with historical controls. Third, quantitative analysis was not performed in an independent core laboratory; however, analysis was performed by experienced cardiologists blinded to angiographic and clinical outcomes. Fourth, not all the patients underwent follow-up angiography (65.5% overall).

Conclusion

Clinical and angiographic data in this study suggest that PES are more effective compared with SES in reducing restenosis and TLR in hemodialysis patients.

References

1. Roiron C, Sanchez P, Bouzamondo A, Lechat P, Montalescot G (2006) Drug eluting stents: an updated meta-analysis of randomised controlled trials. Heart 92:641–649
2. Morice MC, Serruys PW, Sousa JE, Fajadet J, Hayashi EB, Perin M, Colombo A, Schuler G, Barragan P, Guagliumi G, Molnar F, Falotico R (2002) A randomized comparison of a sirolimus-eluting stent with a standard stent for coronary revascularization. N Engl J Med 346:1773–1780
3. Naidu SS, Selzer F, Jacobs A, Faxon D, Marks SD, Johnston J, Detre K, Wilensky RL (2003) Renal insufficiency is an independent predictor of mortality after percutaneous coronary intervention. Am J Cardiol 92:1160–1164
4. Lemos PA, Arampatzis CA, Hoye A, Daemon J, Andrew TL, Ong AT, Saia F, Giessen WJ, McFadden EP, Sianos G, Smits PC, Feyter P, Hofma SH, Domburg RT, Serruys PW (2005) Impact of baseline renal function on mortality after percutaneous coronary intervention with sirolimus-eluting stents or bare metal stents. Am J Cardiol 95:167–172
5. Jeong YH, Hong MK, Lee CW, Park DW, Kim YH, Kim JJ, Park SW, Park SJ (2008) Impact of significant chronic kidney disease on long-term clinical outcomes after drug-eluting stent versus bare metal stent implantation. Int J Cardiol 125:36–40
6. Rosenbulum MA, Robbins MJ, Farkouh ME, Winston JA, Kim MC (2009) Diminished benefits of drug-eluting stents versus bare metal stents in patients with severe renal insufficiency. Nephron Clin Pract 113:c198–c202
7. Nakai S, Masakane I, Shigematsu T, Hamano T, Yamagata K, Watanabe Y, Itami N, Ogata S, Kimata N, Shinoda T, Shouji T, Suzuki K, Taniguchi M, Tsuchida K, Nakamoto H, Nishi S, Nishi H, Hashimoto S, Hasegawa T, Hanafusa N, Fujii N, Marubayashi S, Morita O, Wakai K, Wada A, Iseki K, Tsubakihara Y (2009) An overview of regular dialysis treatment in Japan (as of 31 December 2007). Ther Apher Dial 13:457–504
8. Yasuda K, Kasuga H, Aoyama T, Takahashi H, Toriyama T, Kawade Y, Iwashima S, Yamada S, Kawahara H, Maruyama S, Yuzawa Y, Ishii H, Murohara T, Matsuo S (2006) Comparison of percutaneous coronary intervention with medication in the treatment of coronary artery disease in hemodialysis patients. J Am Soc Nephrol 17:2322–2332
9. Yachi S, Tanabe K, Tanimoto S, Aoki J, Nakazawa G, Yamamoto H, Otsuki S, Yagishita A, Kishi S, Nakano M, Taniwaki M, Sasaki S, Nakajima H, Mise N, Sugimoto T, Hara K (2009) Clinical and angiographic outcomes following percutaneous coronary intervention with sirolimus-eluting stents versus bare-metal stents in hemodialysis patients. Am J Kidney Dis 54:299–306
10. Okada T, Hayashi Y, Toyofuku M, Imazu M, Otsuka M, Sakuma T, Ueda H, Yamamoto H, Kohno N (2008) One-year clinical

outcomes of dialysis patients after implantation with sirolimus-eluting coronary stents. Circ J 72:1430–1435
11. Ishio N, Kobayashi Y, Takebayashi H, Iijima Y, Kanda J, Nakayama T, Kuroda N, Gregorio J, Kouno Y, Suzuki M, Haruta S, Komuro I (2007) Impact of drug-eluting stents on clinical and angiographic outcomes in dialysis patients. Circ J 71:1525–1529
12. Aoyama T, Ishii H, Toriyama T, Takahashi H, Kasuga H, Murakami R, Amano T, Uetani T, Yasuda Y, Yuzawa Y, Maruyama S, Matsuo S, Matsubara T, Murohara T (2008) Sirolimus-eluting stents vs bare metal stents for coronary intervention in Japanese patients with renal failure on hemodialysis. Circ J 72:56–60
13. Ryan TJ, Faxon DP, Gunnar RM, Kennedy JW, King SB, Loop FD, Peterson KL, Reeves TJ, Williams DO, Winters WL (1988) Guidelines for percutaneous transluminal coronary angioplasty: a report of the American College of Cardiology/American Heart Association Task Force on Assessment of Diagnostic and Therapeutic Cardiovascular Procedures (Subcommittee on Percutaneous Transluminal Coronary Angioplasty). Circulation 78:486–502
14. der Zwet PM, Pinto IM, Serruys PW, Reiber JH (1990) A new approach for the automated definition of path lines in digitized coronary angiograms. Int J Card Imaging 5:75–83
15. Cutlip DE, Windecker S, Mehran R, Boam A, Cohen DJ, Es GA, Steg PG, Morel M, Mauri Laura Vranckx P, McFadden E, Lansky A, Hamon M, Krucoff MW, Serruys PW (2007) Clinical end points in coronary stent trials: a case for standardized definitions. Circulation 115:2344–2351
16. Mehran R, Dangas G, Abizaid AS, Mintz GS, Lansky AJ, Satler LF, Pichard AD, Kent KM, Stone GW, Leon MB (1999) Angiographic patterns of in-stent restenosis: classification and implications for long-term outcome. Circulation 100:1872–1878
17. Kasai T, Miyauchi K, Kajimoto K, Kubota N, Kurata T, Hiroyuki Daida (2008) Influence of diabetes on >10-year outcomes after percutaneous coronary intervension. Heart Vessels 23:149–154
18. Rajagopalan S, Dellegrottaglie S, Furniss AL, Gillespie BW, Satayathum S, Lameire N, Saito A, Akiba T, Jadoul M, Ginsberg N, Keen M, Port FK, Mukherjee D, Saran R (2006) Peripheral arterial disease in patients with end-stage renal disease observations from the Dialysis Outcomes and Practice Patterns Study (DOPPS). Circulation 114:1914–1922
19. Wu IW, Hung MJ, Chen YC, Hsu HJ, Chemg WJ, Chang CJ, Wu MS (2010) Ventricular function and all-cause mortality in chronic kidney disease patients with angiographic coronary artery disease. J Nephrol 23:181–188
20. Dibra A, Kastrati A, Mehilli J, Pache J, Schühlen H, von Beckerath N, Ulm K, Wessely R, Dirschinger J, Schömig A (2005) Paclitaxel-eluting or sirolimus-eluting stents to prevent restenosis in diabetic patients. N Engl J Med 353:663–670
21. Windecker S, Remondino A, Eberli FR, Juni P, Raber L, Wenaweser P, Togni M, Billinger M, Tüller D, Seiler C, Roffi M, Corti R, Sütsch G, Maier W, Lüscher T, Hess OM, Egger M, Meier B (2005) Sirolimus-eluting and paclitaxel-eluting stents for coronary revascularization. N Engl J Med 353:653–662
22. Schömig A, Dibra A, Windecker S, Mehilli J, de Lezo JS, Kaiser C, Park SJ, Goy JJ, Lee JH, Lorenzo E, Wu J, Jűni P, Pfisterer ME, Meier B, Kastrati A (2007) A meta-analysis of 16 randomized trials of sirolimus-eluting stents versus paclitaxel-eluting stents in patients with coronary artery disease. J Am Coll Cardiol 50:1373–1380
23. Das P, Moliterno DJ, Charnigo R, Mukherjee D, Steinhubl SR, Sneed JD, Booth DC, Ziada KM (2006) Impact of drug-eluting stents on outcomes of patients with end-stage renal disease undergoing percutaneous coronary revascularization. J Invasive Cardiol 18:405–408
24. Hassani SE, Chu WW, Wolfram RM, Kuchulakanti PK, Xue Z, Gevorkian N, Suddath WO, Satler LF, Kent KM, Pichard AD, Weissman NJ, Waksman R (2006) Clinical outcomes after percutaneous coronary intervention with drug-eluting stents in dialysis patients. J Invasive Cardiol 18:273–277
25. Halkin A, Selzer F, Marroquin O, Laskey W, Detre K, Cohen H (2006) Clinical outcomes following percutaneous coronary intervention with drug-eluting vs bare-metal stents in dialysis patients. J Invasive Cardiol 18:577–583
26. Tamekiyo H, Hayashi Y, Toyofuku M, Ueda H, Sakuma T, Okimoto T, Otsuka M, Imazu M, Kihara Y (2009) Clinical outcomes of sirolimus-eluting stenting after rotational atherectomy. Circ J 73:2042–2049
27. Kuriyama N, Kobayashi Y, Nakayama T, Kuroda N, Komuro I (2006) Images in cardiovascular medicine: damage to polymer of a sirolimus eluting stent. Circulation 114:e586–e587
28. Tanigawa J, Barlis P, Mario C (2008) Heavily calcified coronary lesions preclude strut apposition despite high pressure balloon dilatation and rotational atherectomy: in vivo demonstration with optical coherence tomography. Circ J 72:157–160
29. Mahmud E, Bromberg-Marin G, Palakodeti V, Ang L, Creanga D, DeMaria NA (2008) Clinical efficacy of drug-eluting stent in diabetic patients. J Am Coll Cardiol 51:2385–2395
30. Patterson C, Mapera S, Li HH, Madamanchi N, Hilliard E, Lineberger R, Herrmann R, Charles P (2006) Comparative effects of paclitaxel and rapamycin on smooth muscle migration and survival role of AKT-dependant signaling. Arterioscler Thromb Vasc Biol 26:1473–1480
31. Fröbert O, Lagerqvist B, Carlsson J, Lindbäck J, Stenestrand U, James KS (2009) Difference in restenosis rate with different drug-eluting stents in patients with and without diabetes mellitus. J Am Coll Cardiol 53:1660–1667
32. Iakovou I, Schmidt T, Bonizzoni E, Ge L, Sangiorgi GM, Stankovic G, Airoldi F, Chieffo A, Montorfano M, Carlino M, Michev I, Corvaja N, Briguori C, Gerckens U, Grube E, Colombo A (2005) Incidence, predictors, and outcome of thrombosis after successful implantation of drug-eluting stents. JAMA 293:2126–2130

Atherosclerosis 215 (2011) 43–51

Contents lists available at ScienceDirect

Atherosclerosis

journal homepage: www.elsevier.com/locate/atherosclerosis

Eicosapentaenoic acid reduces warfarin-induced arterial calcification in rats

Saeko Kanai[a,b,*], Kenta Uto[b], Kazuho Honda[b], Nobuhisa Hagiwara[a], Hideaki Oda[b]

[a] Department of Cardiology, Tokyo Women's Medical University, 8-1 Kawada-cho, Shinjuku-ku, Tokyo 162-8666, Japan
[b] Department of Pathology, Tokyo Women's Medical University, 8-1 Kawada-cho, Shinjuku-ku, Tokyo 162-8666, Japan

ARTICLE INFO

Article history:
Received 24 July 2010
Received in revised form
16 November 2010
Accepted 1 December 2010
Available online 8 December 2010

Keywords:
Arterial medial calcification
Eicosapentaenoic acid
Macrophage
MMP-9
MCP-1

ABSTRACT

Background: Eicosapentaenoic acid (EPA), a major n-3 polyunsaturated fatty acid, is reported to have various protective effects for cardiovascular disease. However, few studies have focused on the influence of EPA on vascular calcification.

Methods and results: Arterial medial calcification (AMC) was induced by administering warfarin (3 mg/g food) and vitamin K1 (1.5 mg/g food) for 2 weeks in Sprague–Dawley rats (control group), and EPA (1 g/kg/day) was administered for 2 weeks simultaneously with warfarin and vitamin K1 (EPA group) or after initiation of AMC (late EPA group). EPA showed a marked reduction of medial calcification in the EPA group, and showed a similar effect in the late EPA group. Immunohistochemical and RT-PCR analyses showed that EPA lowered the expression of osteogenetic markers, such as osteopontin, alkaline phosphatase and core binding factor-α1 in the aorta. Significant migration of macrophages with expression of matrix-metalloproteinase (MMP)-2 or MMP-9 was observed in the aortic adventitia around calcification. EPA also reduced macrophage infiltration, MMP-9 expression as well as gene expression of monocyte chemotactic protein (MCP)-1.

Conclusions: These observations indicate that EPA attenuates arterial medial calcification through an effect associated with the suppression of MMP-9 activity and inhibition of macrophage infiltration as well as osteogenic protein expression in warfarin-induced rat models.

Vascular calcification plays an important role in the deterioration of cardiovascular disorders. Vascular calcification consists mainly of atherosclerotic intimal calcification and arterial medial calcification (AMC), also known as Mönckeberg's sclerosis. AMC usually occurs independently, unrelated to intimal calcification, and is found frequently in the muscular arteries of the extremities and characterized by diffuse mineral deposition in the media along the elastic fibers. Several epidemiological and clinical observations have shown that medial calcification is correlated with cardiovascular disease, diabetes, and end-stage renal disease [1,2]. Thus, further elucidation of mechanism responsible for medial calcification and new preventive therapy are required.

Although vascular calcification was thought to be a result from passive degeneration, it has been shown to be an active remodeling process resembling osteogenesis or chondrogenesis [3]. In atherosclerotic intimal calcification, there have been various animal models suggesting that intimal calcification is associated with inflammatory factors, such as oxidized lipids, cytokines in monocytes, oxidant stress, and apoptosis of vascular smooth muscle cells (VSMC) [4–6]. However, only a few murine models of AMC have been reported to show that changes in calcium and phosphate levels and elastin degradation by matrix metalloproteinases (MMPs) may affect pathogenesis of AMC [7]. In addition, no preventive therapy for AMC has yet been established despite its clinical significance.

Eicosapentaenoic acid (EPA), a major omega-3 polyunsaturated fatty acid, is contained in fish such as sardines, tuna, and mackerel. There is increasing epidemiological evidence that EPA has various beneficial effects on cardiovascular disease and cardiovascular mortality [8]. Although the mechanisms are not fully defined, several possible protective effects are considered as follows; attenuation of lipid metabolism, lowering of blood pressure, improvement of vascular endothelial function, reduction of neutrophil and monocyte cytokine production, inhibition of thrombogenesis and the inflammatory response, and an antiarrhythmic effect [9,10]. The significant association between cardiovascular mortality and vascular calcification [1,2] might suggest the possibility that one of the reasons for the inhibitory effect of EPA on cardiovascular disease is attenuation of vascular calcification.

* Corresponding author at: Department of Cardiology, Tokyo Women's Medical University, 8-1 Kawada-cho, Shinjuku-ku, Tokyo 162-8666, Japan. Tel.: +81 3 3353 8111; fax: +81 3 5269 7473.
E-mail address: saeko@research.twmu.ac.jp (S. Kanai).

0021-9150/$ – see front matter © 2010 Elsevier Ireland Ltd. All rights reserved.
doi:10.1016/j.atherosclerosis.2010.12.001

In order to assess the influence of EPA on vascular calcification, especially AMC, we used a rat model of vascular calcification induced by warfarin to block vitamin K-epoxide reductase [11]. This treatment leads to the exhaustion of the vitamin K stores and to inhibit carboxylation of the matrix Gla protein (MGP), an inhibitor of vascular calcification. Vitamin K1, which cannot counteract the effect of warfarin in extra hepatic tissues [12], was also administered to prevent bleeding.

In this study, we demonstrated a significant inhibition of EPA on AMC and also showed that EPA decreased osteogenesis-related gene expression and adventitial macrophage infiltration with MMP-9 in the calcified aorta.

1. Methods

1.1. Materials

Male Sprague–Dawley rats were purchased from Clea Japan, Inc. (Tokyo, Japan). Vitamin K-deficient food without fish flour (3.8 kcal/g) was purchased from Oriental Yeast Co., Ltd. (Tokyo, Japan). Warfarin and vitamin K1 (phylloquinone) were provided by Eisai Co., Ltd. (Tokyo, Japan). Ultra-pure eicosapentaenoic acid ethylester (EPA; >99% purity) was received from Mochida Pharmaceutical Co., Ltd. (Tokyo, Japan).

1.2. Induction of vascular calcification in rats and EPA treatments

To induce vascular calcification, 7-week-old, male Sprague–Dawley rats were given a diet containing warfarin (3 mg/g food) and vitamin K1 (1.5 mg/g food) for 2 weeks (control group, $n=27$). In additional rats, EPA (1 g/kg/day) was given orally using the gavage method in addition to warfarin and vitamin K1 for 2 weeks (EPA group, $n=27$). To examine whether EPA can reduce AMC in secondary prevention, another group of 7-week-old rats ($n=10$) were treated with warfarin and vitamin K1 for 2 weeks, then half of the group was given EPA orally for another 2 weeks especially for histological evaluation (late EPA group, $n=5$).

Rats were killed by exsanguination while under ether anesthesia, and the aortas were removed from the aortic arch, most proximal to the heart, to the femoral artery for later studies. Body weight was measured prior to the experiment and immediately before euthanasia. All animal experiments were approved by the Institutional Animal Care and Use Committee of Tokyo Women's Medical University.

1.3. Measurement of biochemical parameters

Blood samples were collected from the right atrium and centrifuged at 3000 rpm for 30 min to separate the plasma. Each of the parameters was measured with an auto-analyzer (SRL, Tokyo, Japan).

1.4. Histology and immunohistochemistry

The aorta was fixed with 20% neutral buffered formalin for 24 h, then embedded in paraffin, cut into serial sections of 5 μm longitudinally, deparaffinized and stained with hematoxylin–eosin (HE) and elastica van Gieson (EvG). In order to assess the calcified area, longitudinal sections of the aorta were stained for minerals using the von Kossa method. The calcified area was measured at the abdominal aorta (4 mm in length, directly above the bifurcation) and at the common iliac artery (8 mm in length, directly below the bifurcation) and expressed as the percentage of total surface area using the public domain Scion Image program (Scion Corporation, http://www.scioncorp.com/). The numbers of macrophages were counted at the same area as the calcification measurement site.

For immunohistochemical analysis of osteopontin (OPN), MMP-2, MMP-9, and CD68, formalin-fixed paraffin embedded materials were used and antigen retrieval was achieved by boiling in citrate buffer (pH 6.0). For immunohistochemical analysis of alkaline phosphatase (ALP) and monocyte chemotactic protein (MCP)-1, fresh specimens of the aorta were embedded in OCT compound and immediately frozen in liquid nitrogen, cut 3 μm in thickness, fixed in acetone. These sections were then incubated in blocking serum, and incubated overnight at 4 °C with primary antibodies. The sections incubated with primary antibody against MMP-9 were followed by staining with peroxidase-conjugated anti-goat IgG (1:1000) for 1 h and detected using the EnVision plus kit (Dako, Tokyo, Japan). For immunofluorescence, anti-mouse (for OPN, ALP, and CD68), anti-goat (for MCP-1), and anti-rabbit (for MMP-2 and MMP-9) secondary antibodies conjugated to FITC (1:1000, Jackson Laboratories) were applied for 1 h at room temperature. The primary antibodies used in this study were as follows: OPN (1:300, Santa Cruz), ALP (1:100, R and D systems), CD68 (1:300, CHEMICON), MCP-1 (1:300, Santa Cruz), MMP-2 (1:100, Abcam), MMP-9 (1:100, Santa Cruz).

1.5. Reverse transcriptase polymerase chain reaction

The aortas were removed and immediately placed in RNA*later* (Qiagen, Tokyo, Japan) at 4 °C. Total RNA was obtained using a RNeasy Mini kit (Qiagen) and reverse transcribed in 20 μl volumes using an Omnisctipt RT kit (Qiagen) with 1 μl of random primers. Reverse transcriptase polymerase chain reaction (RT-PCR) was performed with the following primers: *OPN*, 5′-CTGCCAGCACACAAGCAGAC-3′ (forward), 3′-TCTGTGGC ATCGGGATACTG-5′ (reverse); *Core binding factor-α1 (Cbfa1)*, 5′-GAGCTACGAAATGC CTCTGC-3′ (forward), 3′-GGACCGTCCACTGTCACTTT-5′ (reverse); *ALP*, 5′-GGACTG GTACTCGGACAATGA-3′ (forward), 3′-CTGGCCTTCTCATCCAGTTC-5′ (reverse); *GAPDH*, 5′-GAGCTACGAAATGCCTCTGC-3′ (forward), 3′-GGACCGTCCACTGTCACTT T-5′ (reverse). Commercial primer pairs (mouse/rat JE/MCP-1/CCL2 primer pair, 246 bp; R and D systems, MN) were used for MCP-1. mRNA was standardized against the level of the respective GAPDH. Band intensities were evaluated using Image Gauge software (Fujifilm, Tokyo, Japan).

1.6. Western blotting

Frozen aorta specimens were homogenized in lysis buffer (50 mM Tris–HCl, pH 7.5, containing 105 mM NaCl, 1% NP-40, 1% sodium deoxycholate, 0.1% SDS and 2 mM EDTA) using Tissue Lyser (Qiagen) and centrifuged at 14,000 rpm for 30 min. 300 μg of protein from each sample was suspended in a loading buffer, separated on a 10% polyacrylamide gel (Readygels J, BIO-RAD, Tokyo, Japan) , and electrophoretically transferred to a nitrocellulose membrane. After blocking the membranes with 2.5% non-fat milk in PBS for 2 h at room temperature, the primary antibody was applied overnight at room temperature. Membranes were then washed with TBS–Tween and incubated with horseradish peroxidase-conjugated goat anti-mouse immunoglobulins secondary antibody (Dako, Japan) for 1 h at room temperature. After washing, membranes were developed by enhanced chemiluminescence with SuperSignal kit according to the manufacturer's instructions (Thermo Fisher Scientific, Inc.) The primary antibodies were MMP-2 and MMP-9 (1:300, Daiichi Fine Chemical). Quantification was performed with relative density employing Image Gauge software.

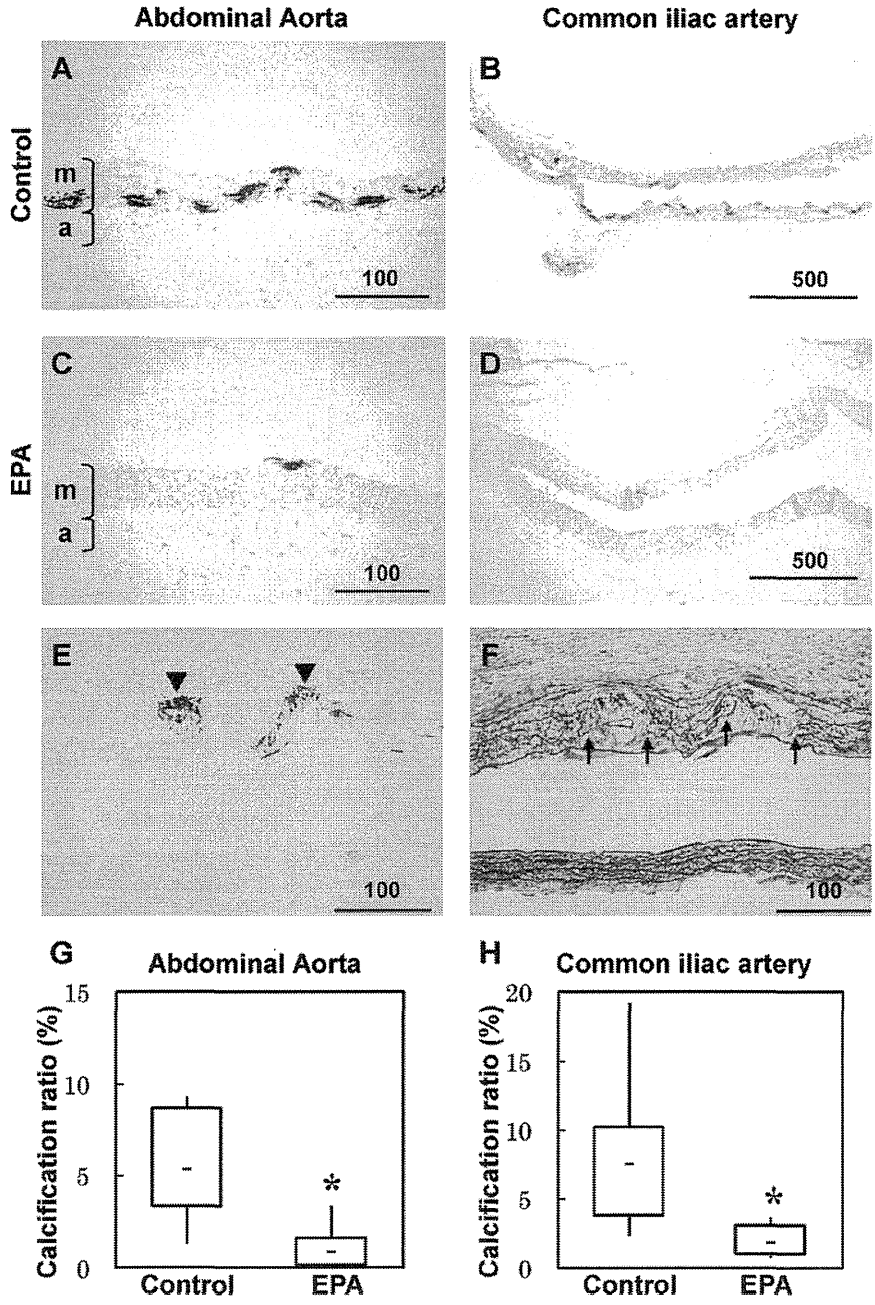

Fig. 1. Inhibitory effects of EPA on warfarin-induced arterial medial calcification. (A–D) von Kossa stained sections of abdominal aorta (A and C) and common iliac artery (B and D) from control (A and B) and EPA (C and D) groups. (E and F) Representative pictures of von Kossa stained (E) and elastica van Gieson stained (F) sections of the calcified aorta. E and F are serial sections. Calcification is shown by a triangle (▲) and elastin degradation was shown by an arrow (↑). (G and H) Quantitative analysis of calcified area in the abdominal aorta (G) and in the common iliac artery (H) ($n = 6$ per group). m, media; a, adventitia. Scale bar, 100 μm (A, C, E and F); 500 μm (B and D). *$p < 0.05$.

1.7. MMP activity

MMP-2 and MMP-9 activities were measured by zymography electrophoresis using a Gelatin Zymo Electrophoresis kit (Life Laboratory Company, Japan) according to the manufacturer's instructions. SDS-polyacrylamide gels were incubated for 24 h at 37 °C. Active MMP-2 and MMP-9 were localized at 45 kDa and 68 kDa, respectively, and visualized as areas of white lytic bands on an otherwise blue background. Gel was digitally photographed and bands were quantified using Image Gauge software.

1.8. Statistics

All data are reported as means ± SD. Means were compared using the Mann–Whitney's *U*-test using the SPSS program, version 13.0J for windows (SPSS Inc., Tokyo, Japan). $p < 0.05$ was considered to indicate a statistically significant difference.

Table 1
Biochemical parameters and body weight gain. Data are shown as means ± SD. Significant differences were analyzed by Mann–Whitney's *U*-test. $^{*}p < 0.01$; $^{**}p < 0.001$ vs. control.

	Control ($n = 14$)	EPA ($n = 14$)
Total cholesterol (mg/dl)	89.1 ± 13.0	71.9 ± 9.9*
Triglyceride (mg/dl)	100.4 ± 44.3	79.1 ± 35.4
Alkaline phosphatase (IU/l)	959.4 ± 244.9	940.9 ± 189.5
Creatinine (mg/dl)	0.25 ± 0.03	0.24 ± 0.03
Calcium (mg/dl)	12.4 ± 0.8	12.2 ± 0.7
P (mg/dl)	16.3 ± 4.6	15.7 ± 3.6
EPA/AA ratio	0.04 ± 0.16	0.58 ± 0.28**
Body weight gain (g)	79.1 ± 10.9	74.6 ± 13.3

* $p < 0.01$.
** $p < 0.001$.

2. Results

2.1. EPA inhibits warfarin-induced arterial medial calcification

After treatment with warfarin for 2 weeks, von Kossa staining of the aortas revealed the presence of extensive arterial medial calcification throughout the abdominal aorta (Fig. 1A) and common iliac arteries (Fig. 1B) in control rats. EvG staining analysis revealed that calcification is associated with the medial elastic fibers, which showed disorganization and fragmentation (Fig. 1E and F). In contrast, EPA reduced arterial medial calcification significantly in the abdominal aorta (histological calcification ratio: control vs. EPA = 5.6 ± 3.4% vs. 1.1 ± 1.3%, $p < 0.05$, $n = 6$; Fig. 1C and G) and in the iliac arteries (control vs. EPA = 8.3% ± 6.2 vs. 1.9 ± 1.5%, $p < 0.05$, $n = 6$; Fig. 1D and H). EPA also blunted degeneration of the elastic network. The EPA/arachidonic acid ratio significantly increased in EPA rats (control vs. EPA = 0.04 ± 0.16 vs. 0.58 ± 0.28, $p < 0.01$, $n = 14$; Table 1). EPA reduced the total cholesterol level (control vs. EPA = 89.1 ± 13.0 vs. 71.9 ± 9.9 mg/dl, $p < 0.01$, $n = 14$; Table 1) and tended to decrease triglyceride level (control vs. EPA = 100.4 ± 44.3 vs. 79.1 ± 35.4 mg/dl, $p = 0.19$; Table 1). To examine the effects of EPA on AMC in secondary prevention, we also assessed whether EPA reduces preformed AMC by administering EPA for 2 weeks after treatment with warfarin and vitamin K1 for 2 weeks. Histological analysis showed that EPA significantly decreased AMC in abdominal aorta (histological calcification ratio: control vs. EPA = 5.4 ± 3.2% vs. 1.4 ± 1.6%, $p < 0.05$, $n = 5$; supplemental Fig. A). Although it was not statistically significant, EPA showed a reduction tendency in common iliac artery (control vs. EPA = 7.6 ± 2.0% vs. 5.5 ± 2.7%, $p = 0.22$, $n = 6$; supplemental Fig. B).

2.2. EPA attenuates osteogenetic markers in the calcified aorta

It has been reported that osteogenetic processes are involved in AMC, and bone-associated proteins are expressed around calcified lesions [3,7]. Therefore, we examined the osteogenic phenotype of calcified arteries in this model. Immunohistochemical analysis revealed that OPN, a glycosylated phosphoprotein associated with mineral deposit [13], was expressed in the calcified lesions in the aorta (Fig. 2A). Similarly, ALP, a functional phenotypic marker of osteoblast [14], was observed in the calcified vascular smooth muscle cells (Fig. 2B). RT-PCR analysis revealed that the mRNA expressions of these osteoblastic markers and Cbfa1, a key transcription factor of osteoblastic differentiation, were significantly downregulated in the EPA rats (OPN, $p < 0.05$, n = 6; ALP, $p < 0.01$, $n = 6$; Cbfa1, $p < 0.05$, $n = 6$; Fig. 2C–F). These results suggest that the process similar to osteogenesis, is implicated in the development of medial calcification in this model, and EPA attenuates this process.

2.3. EPA reduces adventitial macrophage infiltration in the calcified aorta

Prior studies showed that MMP-2 and MMP-9 bind to insoluble elastin playing an important role in elastinolysis leading to the initiation of vascular calcification [15,16]. In fact, disorganization and fragmentation of elastic fibers were observed in the calcified artery of rats treated with warfarin. Although MMPs are secreted from various cells, such as immune cells, fibroblasts, endothelial cells, and smooth muscle cells, macrophages, in particular, have been reported for their involvement in vascular calcification [17,18]. Therefore, we assessed whether macrophages correlate with medial calcification. Immunohistochemistry for CD68 revealed that numerous macrophages migrated into the aortic adventitia around the calcified lesion in control rats (Fig. 3A and C). Macrophages were found not only around progressive calcified areas (supplemental Fig. C and D) but also around extremely small calcifications in the early stage (supplemental Fig. E and F). On the other hand, such significant macrophage infiltration was not observed in the non-calcified aorta (Fig. 3B and D). EPA decreased adventitial macrophages infiltration significantly (abdominal aorta, control vs. EPA = 14.5 ± 6.3 vs. 4.7 ± 2.6/mm, $p < 0.01$, $n = 6$; iliac artery, control vs. EPA = 15.5 ± 7.3 vs. 5.2 ± 1.7/mm, $p < 0.01$, $n = 5$ or 6; Fig. 3G), showing a positive correlation between the number of macrophages and the calcification ratio ($p < 0.01$, $r = 0.79$, $n = 12$; Fig. 3H). Furthermore, some of these adventitial macrophages around the calcified lesions showed positive immunohistochemical staining for MMP-2 (Fig. 3E) or MMP-9 (Fig. 3F). VSMC around the calcification also showed immunoreactivity of MMP-2 (Fig. 3E). These findings suggest that macrophages are an important source for MMP-2 and MMP-9, associated with the development of medial calcification.

2.4. Effects of EPA on MMP expressions in the aorta

To investigate protease expressions in the aorta, a Western blot analysis was performed for MMP-2 and MMP-9. As shown in Fig. 3A, EPA markedly decreased MMP-9 expression in the aorta compared with that of control rats ($p < 0.01$, $n = 5$; Fig. 4C), whereas MMP-2 expression showed no significant difference between the groups (Fig. 4A and B). Similarly, gelatin zymography on aortic extracts revealed a decrease in MMP-9 activity in EPA rats compared with that of control rats ($p < 0.05$, $n = 6$; Fig. 4D and F). On the contrary, direct effect of EPA on active MMP-2 expression was not clear (Fig. 4D and E). These findings indicate that activation of MMP-9 is associated with pathogenesis of medial calcification in this study.

2.5. EPA attenuates MCP-1 expressions in the calcified aorta

We then accessed MCP-1, a chemokine which recruits and activates monocyte/macrophage from the circulation to inflammatory sites. MCP-1 is secreted from various cells, such as fibroblasts, endothelial cells, VSMC, and macrophage. Immunohistochemistry for MCP-1 revealed colocalization with macrophages in adventitia (Fig. 5A) and also expressed in VSMC around sites of calcification in the control group, although the expression of MCP-1 decreased in the EPA group (Fig. 5B). The MCP-1 mRNA expression in the aorta was significantly inhibited in EPA rats compared to control rats ($p < 0.01$, $n = 6$; Fig. 5C and D). These observations indicate the possibility that EPA decreases macrophage infiltration through the suppression of MCP-1 expressions in the aorta.

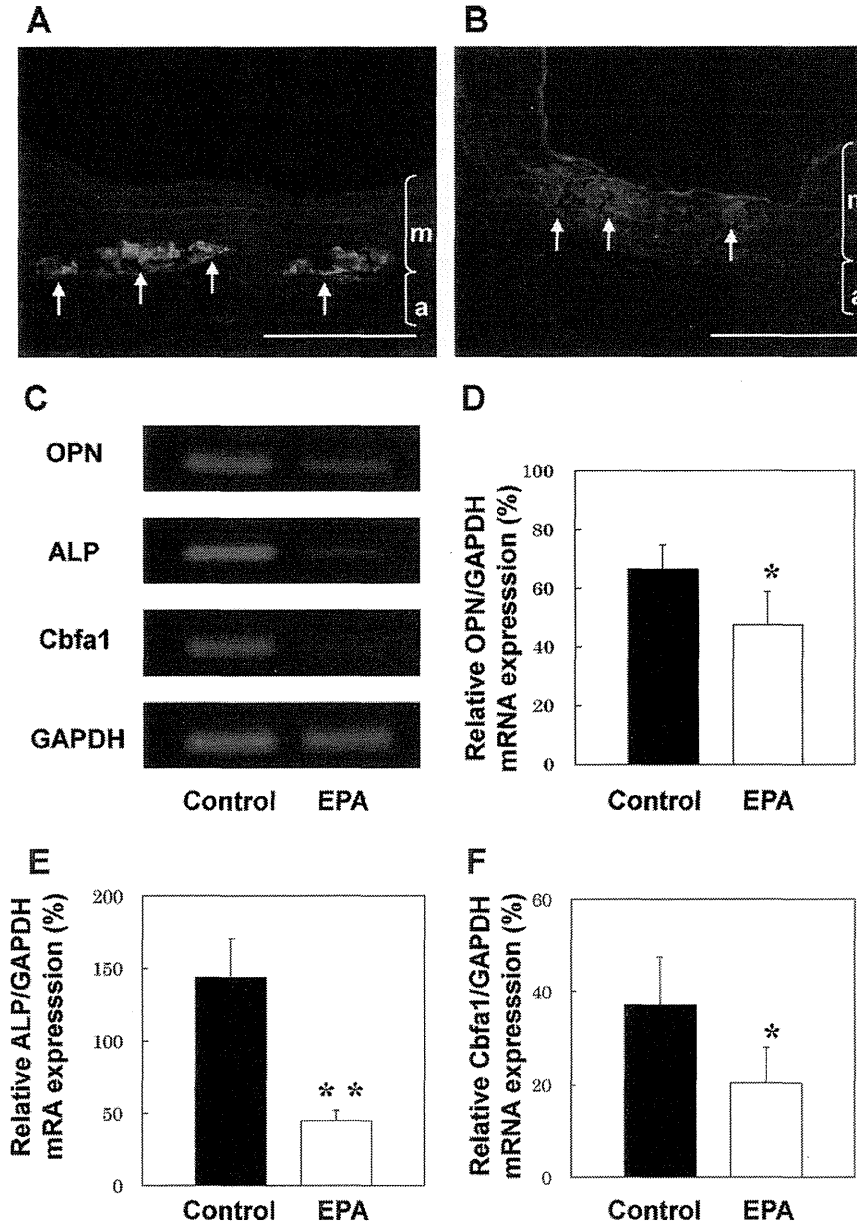

Fig. 2. EPA attenuates osteogenetic signals in the calcified aorta. (A and B) Immunohistochemical detection of osteopontin (OPN) (A) and alkaline phosphatase (ALP) (B) colocalizing with the calcification in the common iliac artery of the control group. Arrows denote areas of positive staining. m, media; a, adventitia. Scale bar, 100 μm. (C) Representative mRNA expressions assessed by RT-PCR. OPN (D), ALP (E), and Cbfa1 (F) mRNA expressions are normalized to GAPDH and evaluated densitometrically ($n=6$ per group). $^{*}p<0.05$, $^{**}p<0.01$.

3. Discussion

We set out to determine whether EPA significantly inhibits AMC and to determine whether EPA decreases osteogenesis-related gene expression and adventitial macrophage infiltration with MMP-9 in the calcified aorta.

The major finding of this present study is that EPA reduces AMC in vivo. We used a warfarin-induced AMC model established by Price in 1998 [11] The mechanism of this model is inhibiting γ-carboxylation of MGP, a calcium-binding and vitamin K-dependent protein that inhibits vascular calcification by antagonizing bone morphogenetic protein and binding elastin. A typical form of morphology of calcifications is linear deposit along the elastic lamina in the abdominal aorta to the iliac arteries a common site of AMC in humans, and those lesions progress to massive AMC similar to Mönckeberg's sclerosis without atherosclerosis. Although MGP-deficient mice show similar AMC, they have osteogenic disorders and calcification progresses faster than warfarin-treated rats and result in death from aortic rupture within 6 weeks [19]. Therefore, it is difficult to use MGP-deficient mice for suppression experiments of AMC. There have been other murine models to study inhibition of vascular calcification such as treating low-density lipoprotein receptor (LDL)-deficient mice or apolipoprotein E-deficient mice with high-fat or high-phosphate diet combined nephrectomy [5,17,20]. However, mainly intimal calcification occurs in these models and its pathogenesis is complicated. Although periadventitial application of $CaCl_2$, which causes medial calcification, has also been used in several studies [15], it requires surgery. In this

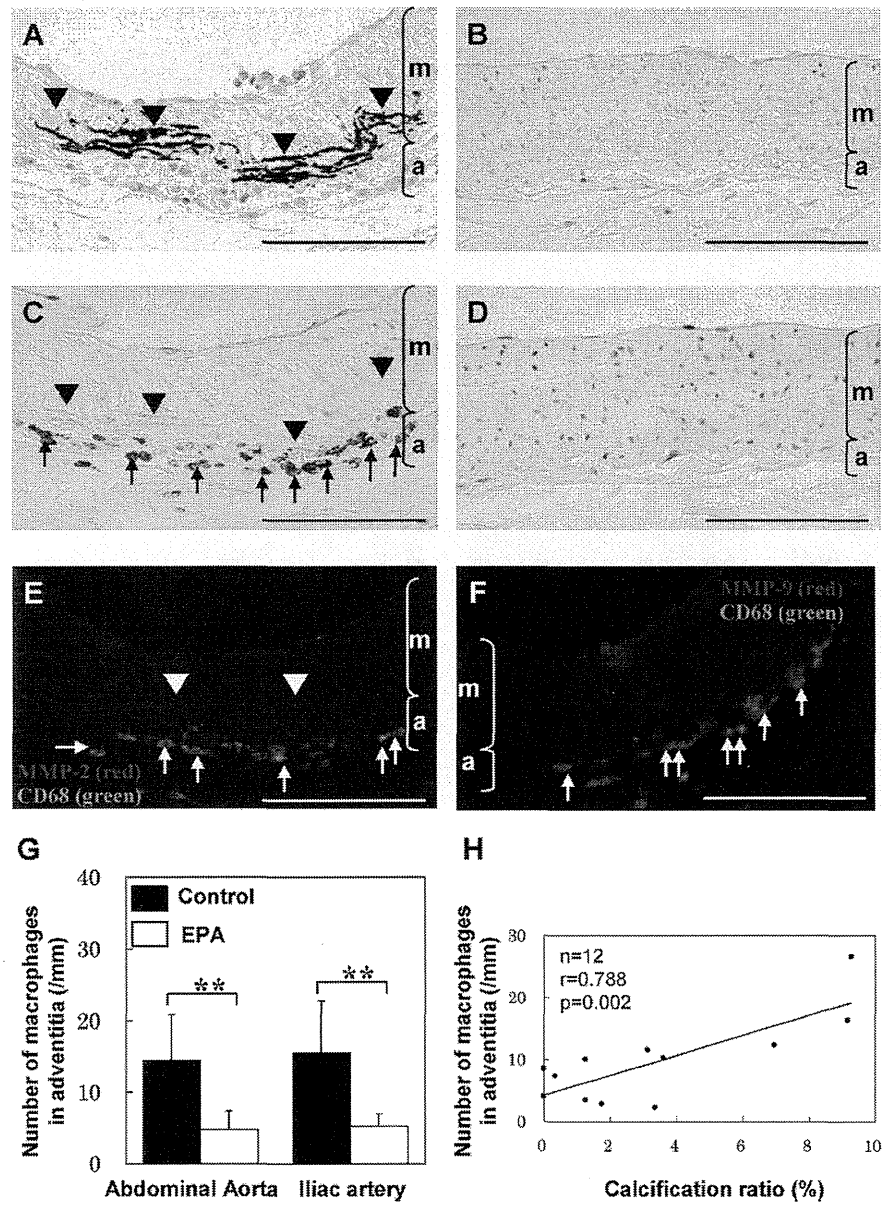

Fig. 3. EPA suppresses adventitial macrophage infiltration in rats treated with warfarin. (A–D) von Kossa stained sections (A and B) and immunostaining for CD68 (C and D) of the calcified common iliac artery (A and C) and non calcified common iliac artery (B and D) of rats in the control (A and C) or EPA (B and D) group. Numerous macrophages showing positive staining for CD68 (arrows) were found in adventitia correlated with medial calcified area (arrow heads, A and C), but not around non-calcified lesions (D). (E and F) Co localization of MMP-2 (red) and CD68 (green) (E) and MMP-9 (red) and CD68 (green) (F) in adventitia along medial calcification of common iliac artery of rat in the control group. Arrows indicate macrophages double positive for MMP-2 and CD68 (E) and MMP-9 and CD68 (F). Arrow heads indicate VSMC positive for MMP-2 (E). (G) Quantitative evaluations of macrophages positive for CD68 in adventitia ($n=5$ in the iliac artery of the control group. $n=6$ in others). (H) Correlation between number of macrophages and calcification ratio of abdominal aorta in both control and EPA groups ($n=12$). A, C, E and F, B and D are serial sections, respectively. m, media; a, adventitia. Scale bar, 100 μm. $^{**}p<0.01$. (For interpretation of the references to color in this figure legend, the reader is referred to the web version of the article.)

study, warfarin treatment requires only 2 weeks to induce calcification, and provides less-invasive and highly reproducible model of AMC. For this reason, it has been used in several preventive AMC experiments [21,22].

ω-3 PUFA has pleiotropic effects and has been shown to decrease the risk of major cardiovascular events, such as myocardial infarction [23], sudden cardiac death [24], arrhythmias [25], and death in patients with heart failure [26]. Recent large randomized trials have documented that EPA reduced the incidence of major coronary events in patients with hyperlipidemia without affecting serum LDL cholesterol [27]. Although detailed action mechanisms of EPA have not been clarified, 2 basic mechanisms, the effects on atherothrombosis and ion channels, are thought to be important. However, there have been few reports on the effects of EPA in vascular calcification, much less AMC.

AMC has demonstrated similar processes to intramembranous bone formation, unlike intimal calcification, which forms via a process similar to endochondral ossification [3]. Our finding that EPA decreased the expressions of osteogenetic markers in the aorta indicates that suppression of AMC by EPA might occur via inhibiting transition of VSMC into osteoblast-like cells. However, EPA was reported to have opposite effects on osteoblast, increasing osteo-

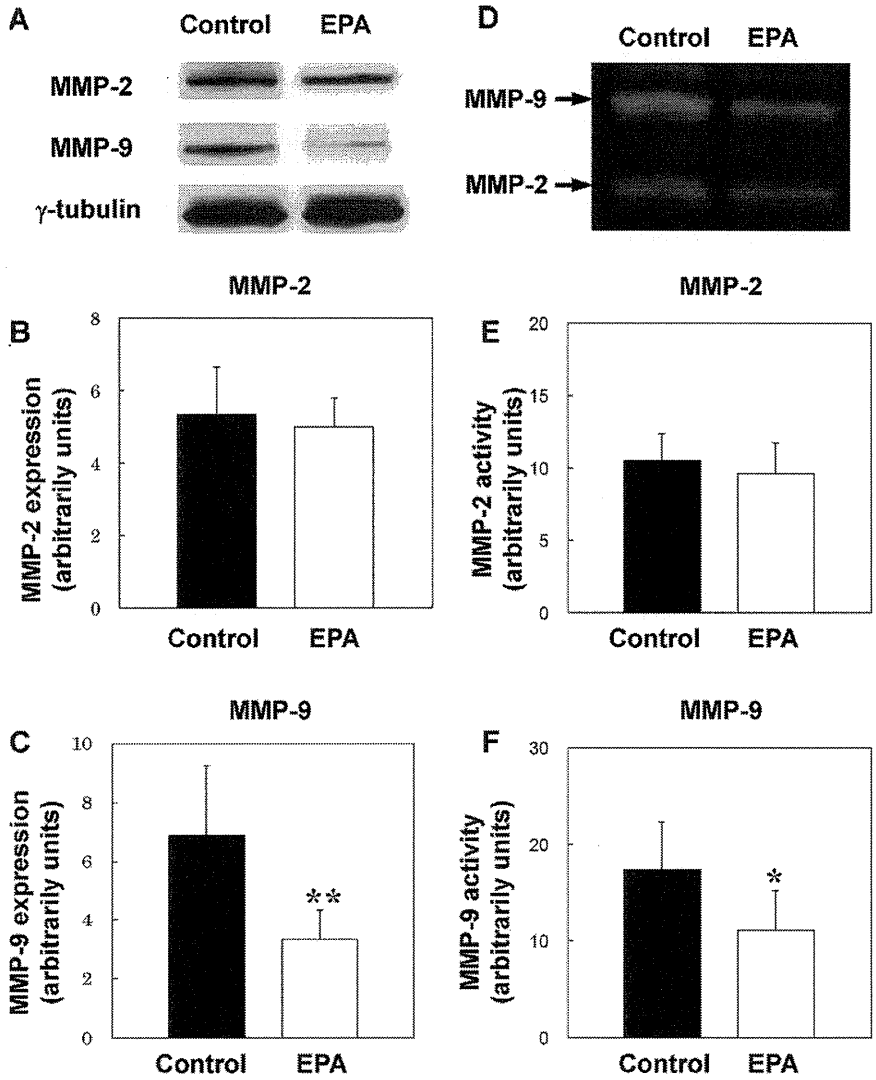

Fig. 4. Inhibitory effects of EPA on MMP expressions in the aorta. (A and D) Representative MMP-2 and MMP-9 levels in the aorta assessed by Western blotting (A, $n=5$ per group) and gelatin zymography (D, $n=6$ per group). Protein expressions of MMP-2 (B) and MMP-9 (C), and enzyme activity of MMP-2 (E) and MMP-9 (F) were evaluated by densitometry and expressed as arbitrarily units. $^{*}p<0.05$, $^{**}p<0.01$.

genetic activity and prevention of loss of bone mineral density [28]. There seems to be a difference in the effect of EPA on osteoblast-like VSMC and osteoblast in the bone. Our findings are supported by in vitro observations that EPA inhibited osteoblastic differentiation and mineralization of vascular cells by managing the p38-MAPK and PPAR-γ pathways [29]. Furthermore, Schlemmer reported that EPA reduced calcium glubionate-induced ectopic calcification of rat aortas [30].

This osteoblast-like phenotypical change of VSMC is speculated to follow after preceding elastin degradation and activation of MMP-2 and transforming growth factor (TGF)-β [31]. Our results that calcium deposition was localized in elastic fibers with elastin degeneration and MMP-9 elevation agree with a previous report that elastase activity and extracellular matrix degradation are essential to the early process of AMC, accompanied by the change of MMP-9 and TGF-β in warfarin-treated rat models [32]. Although the type of elastase which contributes to the pathogenesis of AMC may differ depending on the experimental methodology, inhibiting MMP activity may have important implications for the treatment of AMC [15,16]. We speculate that EPA plays an inhibitory role mainly in the early process of AMC through suppressing MMP activity. In addition, EPA may also have some benefits in secondary prevention of AMC as shown by the results of late EPA group.

Inflammation may be an important contributor to vascular calcification [5], especially, as macrophages contribute to elastin degeneration and vascular calcification via expressing elastase such as MMPs and cathepsin S [17], and TNF-α, a pleiotropic cytokine that is reported to promote osteoblastic differentiation of VSMC [18]. One striking result of our study was the presence of numerous macrophages in adventitia around both tiny calcification in early stage and progressive calcification. Moreover, some of these macrophages expressed MMP-2 and MMP-9. These observations indicate that adventitial macrophage may play an important role in the process of AMC. Furthermore, EPA also inhibited MCP-1, a chemokine inducing recruitment of monocytes, which was detected in VSMC and adventitial macrophages. Taken together, suppression of macrophage infiltration into adventitia via inhibition of MCP-1 might be in part responsible for the effect of EPA on AMC. Further studies are needed to clarify the role of macrophages in the pathogenesis of AMC.